NASA TECHNICAL MEMORANDUM

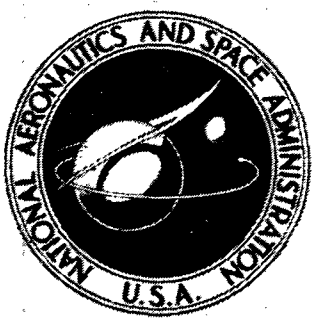

NASA TM X-2674

NASA TM X-2674

EFFECTS OF WING-PIVOT LOCATION AND FOREWING CONFIGURATION ON THE LOW-SPEED AERODYNAMIC CHARACTERISTICS OF A VARIABLE-SWEEP AIRPLANE MODEL

by Jarrett K. Huffman

Langley Research Center
Hampton, Va. 23365

NATIONAL AERONAUTICS AND SPACE ADMINISTRATION • WASHINGTON, D. C. • DECEMBER 1972

1. Report No.	2. Government Accession No.	3. Recipient's Catalog No.
NASA TM X-2674		

4. Title and Subtitle	5. Report Date
EFFECTS OF WING-PIVOT LOCATION AND FOREWING CONFIGURATION ON THE LOW-SPEED AERODYNAMIC CHARACTERISTICS OF A VARIABLE-SWEEP AIRPLANE MODEL	December 1972
	6. Performing Organization Code
7. Author(s)	8. Performing Organization Report No.
Jarrett K. Huffman	L-8026
	10. Work Unit No.
9. Performing Organization Name and Address	760-67-01-01
NASA Langley Research Center Hampton, Va. 23365	11. Contract or Grant No.
	13. Type of Report and Period Covered
12. Sponsoring Agency Name and Address	Technical Memorandum
National Aeronautics and Space Administration Washington, D.C. 20546	14. Sponsoring Agency Code

15. Supplementary Notes

16. Abstract

An investigation has been made to determine the effects of the location of the wing pivot and geometry of the forewing on the static longitudinal aerodynamic characteristics at subsonic speeds of a model representing a variable-sweep supersonic fighter airplane. Results indicate that as the wing-pivot location moves aft and outboard, the change in static margin due to wing sweep is reduced. Increasing the forewing area resulted in a forward shift of the aerodynamic center as well as a slight reduction in the aerodynamic-center variation due to wing sweep.

17. Key Words (Suggested by Author(s))	18. Distribution Statement
Variable sweep Wing-pivot location Longitudinal aerodynamics	Unclassified – Unlimited

19. Security Classif. (of this report)	20. Security Classif. (of this page)	21. No. of Pages	22. Price*
Unclassified	Unclassified	57	$3.00

*For sale by the National Technical Information Service, Springfield, Virginia 22151

EFFECTS OF WING-PIVOT LOCATION AND FOREWING CONFIGURATION ON THE LOW-SPEED AERODYNAMIC CHARACTERISTICS OF A VARIABLE-SWEEP AIRPLANE MODEL

By Jarrett K. Huffman
Langley Research Center

SUMMARY

An investigation has been made to determine the effects of the location of the wing pivot and geometry of the forewing on the static longitudinal aerodynamic characteristics at subsonic speeds of a model representing a variable-sweep supersonic fighter aircraft. Results indicate that as the wing-pivot location moves aft and outboard, the change in static margin due to wing sweep is reduced. Increasing the forewing area resulted in a forward shift of the aerodynamic center as well as a slight reduction in the aerodynamic-center variation due to wing sweep. The model exhibited a large negative pitching-moment coefficient at zero lift which was unaffected by wing-pivot location or forewing configuration. Results also indicate that an available analytical approach predicts with a fair degree of accuracy the effect of pivot location on the shift in wing-fuselage aerodynamic center between the maximum and minimum sweep angles.

INTRODUCTION

The high level of longitudinal stability usually encountered by an aircraft at supersonic speeds as a result of the rearward shift of the wing aerodynamic center can have a serious impact on aircraft turning performance. Variable-sweep wing aircraft can encounter a more severe problem due to the additional rearward movement of the aerodynamic center as the wing is swept back for supersonic flight. References 1 to 7 show that the position of the wing pivot has a dramatic influence on the incremental change of the aerodynamic center between the low and high wing sweep position.

Configurations with outboard wing-pivot designs usually require a forewing or fixed glove area to provide the structure to support the pivot, and the forewing therefore must be considered early in the aircraft design. The forewing must not be excessively large, must not cause handling problems at maneuvering conditions, and must have sufficient sweep to satisfy high-speed stability requirements.

An experimental investigation was made at a Mach number of 0.27 in the Langley 7- by 10-foot high-speed tunnel to determine the effects of systematic variations of the wing-pivot location and the geometry of the forewing on the low-speed static longitudinal aerodynamic characteristics of a model representative of a supersonic fighter aircraft. The present paper presents the results of the investigation along with theoretical predictions of the aerodynamic-center location. Experimental results on the same model at supersonic speeds are reported in reference 8.

SYMBOLS

The forces and moments are presented relative to the stability-axis system. All coefficients are nondimensionalized with respect to the geometric characteristics of a theoretical wing having a 15° leading-edge sweep and straight tapered planform. The theoretical wing was considered to extend into the fuselage center line. The moment reference point was located at fuselage station 0.517 meter (20.341 in.) which corresponded to the $0.16\bar{c}$ location of the wing employing pivot location 1 in the 15° leading-edge sweep condition, which is used as the reference configuration. This moment reference point remains the same for all configurations and wing sweeps. The reference wing span is 0.7465 meter (29.38 in.). All measurements were made in U.S. Customary Units and are presented in both SI and U.S. Customary Units.

$\bar{c}$	mean geometric chord, 0.1093 meter (4.3 in.)
$C_{A,i}$	internal-flow axial-force corrections, $\frac{\text{Axial force}}{qS}$
C_D	drag coefficient, $\frac{\text{Drag}}{qS}$
C_L	lift coefficient, $\frac{\text{Lift}}{qS}$
C_{L_α}	lift-curve slope, $\frac{\partial C_L}{\partial \alpha}$
C_m	pitching-moment coefficient, $\frac{\text{Pitching moment}}{qS\bar{c}}$
C_{m_o}	pitching-moment coefficient at $C_L = 0$
$\frac{\partial C_m}{\partial C_L}$	static margin measured near zero lift
i_t	horizontal-tail deflection angle, deg
M	Mach number

q free-stream dynamic pressure, N/m^2 (lb/ft^2)

S reference wing area, 0.077 $meter^2$ (0.8365 ft^2)

α angle of attack, deg

Λ sweep of the wing leading edge, deg

MODEL

Details of the model are shown in figure 1 and photographs are presented in figure 2. The model was representative of a midwing, variable-sweep fighter configuration with a wing sweep range from 15^o to 70^o utilizing the wing-pivot locations shown in figure 3. Also shown in figure 1 are the three forewing configurations studied and the two longitudinal locations of the inlets. Forewing configuration A is used as the reference configuration, the outlines for configurations B and C being shown as dashed lines.

In the low-sweep positions ($\Lambda = 15^o$), the wing airfoil section was one-half of a NACA 65A024 section (measured normal to the wing leading edge) with a modified leading edge. The section was therefore 12 percent thick, had a flat bottom, and 6-percent chord camber. No geometric twist was incorporated in the movable panel.

The horizontal and vertical tails are shown in figures 1(b) and 1(c), respectively. The airfoil sections of those two surfaces were NACA 65A006 sections. The horizontal tail was all movable and provided deflections from 5^o to -20^o.

The nine wing-pivot locations are shown in figure 3. Wing-pivot locations 1, 2, and 3 were selected to hold the same low-sweep planform while the planform of the high-sweep planform was allowed to vary as the pivot location changes. (See fig. 3(b).) This same variation holds for wing-pivot locations 4, 5, and 6. (See fig. 3(c).) However, this wing-pivot path has a more rearward position than those for wing-pivot-point paths 1, 2, and 3. Wing-pivot locations 1, 7, 8, and 9 (see fig. 3(d)) were designed to maintain the identical high-sweep wing planform and identical low-sweep wing span. However, the longitudinal position of the low-sweep planform varied with pivot point location.

TESTS AND CORRECTIONS

The investigation was made in the Langley high-speed 7- by 10-foot tunnel at a Mach number of 0.27 corresponding to a dynamic pressure of 5034 N/m^2 (105 lb/ft^2) and a Reynolds number of 5.9×10^6 per meter (1.8×10^6 per foot).

Lift, drag, and pitching moment were measured through an angle-of-attack range of -4° to 22°. Corrections due to bending of the sting and balance support system under aerodynamic load have been applied to the angle of attack. The jet-boundary corrections to the angle of attack were applied by the method of reference 9. The effect of model blockage was accounted for by the method of reference 10. The drag data presented are corrected to a condition of free-stream static pressure acting on the base of the model and the balance cavity.

Internal-flow axial-force measurements were made with a rake of total head probes and these data were subtracted from the axial-force data obtained from the strain-gage balance. These corrections are shown in figure 4.

PRESENTATION OF RESULTS

The results of the tests are presented in the following figures:

	Figure
Forewing configuration A:	
Effect of wing sweep and wing-pivot location. $i_t = 0^{\circ}$	5 to 9
Variation of static margin as a function of wing sweep angle for the three wing-pivot paths. $M = 0.27$	10
Effect of horizontal-tail incidence:	
Wing-pivot location 1; $\Lambda = 15^{\circ}$	11
Wing-pivot location 8; $\Lambda = 15^{\circ}$	12
Wing-pivot location 1; $\Lambda = 35^{\circ}$	13
Wing-pivot locations 1, 7, 8, and 9; $\Lambda = 70^{\circ}$	14
Forewing configuration B:	
Effect of wing sweep and wing-pivot location. $i_t = 0^{\circ}$	15 to 19
Forewing configuration C:	
Effect of wing sweep and wing-pivot location. $i_t = 0^{\circ}$	20 to 22
Lift-curve slope and static margin variation for wing-pivot location 8 as a function of wing sweep angle for the three forewing configurations	23
Variation in pitching-moment coefficient as a function of angle of attack for the three forewing configurations and wing-pivot locations 1 and 8. $M = 0.27$	24
A comparison of theoretical and experimental static margin variation with wing sweep angle for wing-pivot locations 1 and 8, horizontal tail off. $M = 0.27$	25

RESULTS AND DISCUSSION

Wing-Pivot Location

Figures 5 to 9 present the basic longitudinal aerodynamic characteristics for configuration A with the various wing-pivot locations and wing sweep angles. The configuration with the wing at 15° sweep in the most forward longitudinal location (pivot location paths 1, 2, and 3) is shown to have marginal stability around zero lift and pitch-up tendencies in the intermediate lift range.

A large negative pitching-moment coefficient at zero lift C_{m_0} is noted in the data of figures 5(a) and 6(a). This effect is primarily associated with the large camber of the outboard wing panel. Although the streamwise camber is reduced and C_{m_0} becomes less negative as the wing sweeps back to 70°, the negative levels are still large. This large negative C_{m_0} requires a relatively large horizontal-tail deflection in order to trim (see figs. 10 to 13), and therefore, reduces the instantaneous control-limited load factor capability of the configuration.

The variation in static margin as a function of wing sweep angle for the pivot locations tested is summarized in figure 10. (The insert in the figure shows the path of the various pivot points.) The smallest variation of static margin (movement of the aerodynamic center) between high- and low-wing sweep angles occurs for the wing in the most outboard wing-pivot locations. Wing-pivot paths 1, 2, and 3 (fig. 10(a)) were selected to hold the same low-sweep wing position while the high-sweep planform is allowed to vary as the pivot location changed. The same concept was used for wing-pivot paths 4, 5, and 6 (fig. 10(b)); however, the low-sweep wing planform had a more rearward location than those for pivot paths 1, 2, and 3. These data show basically the same trends; that is, as the pivot point moves aft and inboard, the static margin increment between the low- and high-sweep wing increased. In each case this increase in static margin was caused by the movable panel carrying a larger percentage of the load and thereby reducing the relative amount carried by the forewing. (See refs. 6 and 11.) Wing-pivot-point paths 1, 7, 8, and 9 (fig. 10(c)) were selected to keep the same low-sweep wing span and the identical high-sweep wing planform. This combination caused the low-sweep wing to move forward as the pivot location moved inboard and forward. (See fig. 3(d).) The data show that as the pivot point moves aft and outboard, the low-sweep static margin increases and the change in static margin from high- to low-wing sweep is reduced. The smallest variation in static margin between the high- and low-wing sweep occurs for pivot location 8. It should be noted that for wing-pivot location 9, the aerodynamic center for the sweptback wing was located forward of the aerodynamic center for the swept forward wing.

Forewing Configuration

Another variable which could have an influence on the position of the aerodynamic center is the geometry of the fixed section of the wing. Basic data obtained with forewings *B* and *C* are presented in figures 15 to 22 and show trends similar to those exhibited by forewing A (figs. 5 to 9). Shown in figure 23 is the lift-curve slope and the static margin (taken near zero lift) as a function of the wing sweep for pivot location 8 for the three forewing configurations. As can be seen from the data, a small increase in lift-curve slope with increasing forewing area is noted. Also the change in aerodynamic center from low- to high-wing sweep is slightly decreased with increasing forewing area.

There was also a decrease in the total level of static margin with increasing forewing area which is to be expected since the area increase was added ahead of the model center of gravity.

Shown in figure 24 is the pitching-moment coefficient C_m as a function of angle of attack for the three forewing configurations and wing-pivot locations 1 and 8. The data indicate a pronounced destabilizing effect with increasing forewing area, a pitch-up tendency at low angles of attack occurring for the larger forewings at low-sweep angles. It should be noted that the large negative C_{m_0} values were generally unaffected by the increasing area of the forewing.

Comparison of Theory With Experiment

Figure 25 shows the static margin estimated by the vortex lattice method (ref. 8) as a function of wing sweep angle Λ for wing-pivot locations 1 and 8 compared with experimental horizontal-tail-off data. Thickness or other body shaping being neglected, the input for the vortex lattice approach (ref. 11) was the outline of the planview of the wing-body configuration (forewing configuration C). The symbols are experimental data points whereas the curves are the results of the vortex lattice approach. Figure 25 indicates that the static margin of this tail-off configuration is predicted very well at the maximum and minimum wing sweep angles.

CONCLUSIONS

An investigation has been made to determine the effect of wing-pivot location and geometry of the forewing on the static longitudinal aerodynamic characteristics at subsonic speeds of a model representing a variable-sweep supersonic fighter aircraft. As a result of this program, several conclusions can be made.

1. As the wing-pivot location moves aft and outboard, the rearward movement of the aerodynamic center from minimum to maximum wing sweep is reduced.

2. Increasing the forewing area resulted in a forward shift of the aerodynamic center but only a small reduction in the aerodynamic-center variation due to wing sweep.

3. This model exhibited a large negative pitching-moment coefficient at zero lift which was essentially unaffected by wing-pivot location or forewing geometry.

4. The vortex lattice approach predicted the effect of pivot location on the shift in wing-fuselage aerodynamic center between minimum and maximum wing sweep angles that agreed well with the experimental data.

Langley Research Center,
National Aeronautics and Space Administration,
Hampton, Va., October 30, 1972.

REFERENCES

1. Alford, William J., Jr.; and Henderson, William P.: An Exploratory Investigation of the Low-Speed Aerodynamic Characteristics of Variable-Wing-Sweep Airplane Configurations. NASA TM X-142, 1959.

2. Alford, William J., Jr.; Luoma, Arvo A.; and Henderson, William P.: Wind-Tunnel Studies at Subsonic and Transonic Speeds of a Multiple-Mission Variable-Wing-Sweep Airplane Configuration. NASA TM X-206, 1959.

3. Spencer, Bernard, Jr.: Stability and Control Characteristics at Low Subsonic Speeds of an Airplane Configuration Having Two Types of Variable-Sweep Wings. NASA TM X-303, 1960.

4. Bielat, Ralph P.; and Robins, A. Warner: Stability and Control Characteristics at Transonic Speeds of Two Variable-Sweep Airplane Configurations Differing in Wing-Pivot Locations. NASA TM X-559, 1961.

5. Foster, Gerald V.; and Morris, Odell A.: Stability and Control Characteristics at a Mach Number of 1.97 of an Airplane Configuration Having Two Types of Variable-Sweep Wings. NASA TM X-323, 1960.

6. Toll, T. A.; Polhamus, E. C.; and Aiken, W. S., Jr.: NASA Variable-Geometry Research. AGARD Rep. 447, Apr. 1963.

7. Lamar, John E.; and Alford, William J., Jr.: Aerodynamic-Center Considerations of Wings and Wing-Body Combinations. NASA TN D-3581, 1966.

8. Campbell, James F.: Stability Characteristics of a Variable-Sweep Lightweight Fighter Configuration With a Keel-Type Fuselage at Mach Numbers From 1.50 to 2.86. NASA TM X-1350, 1967.

9. Gillis, Clarence L.; Polhamus, Edward C.; and Gray, Joseph L., Jr.: Charts for Determining Jet-Boundary Corrections for Complete Models in 7- by 10-Foot Closed Rectangular Wind Tunnels. NACA WR L-123, 1945. (Formerly NACA ARR L5G31.)

10. Herriot, John G.: Blockage Corrections for Three-Dimensional-Flow Closed-Throat Wind Tunnels, With Consideration of the Effect of Compressibility. NACA Rep. 995, 1950. (Supersedes NACA RM A7B28.)

11. Margason, Richard J.; and Lamar, John E.: Vortex-Lattice FORTRAN Program for Estimating Subsonic Aerodynamic Characteristics of Complex Planforms. NASA TN D-6142, 1971.

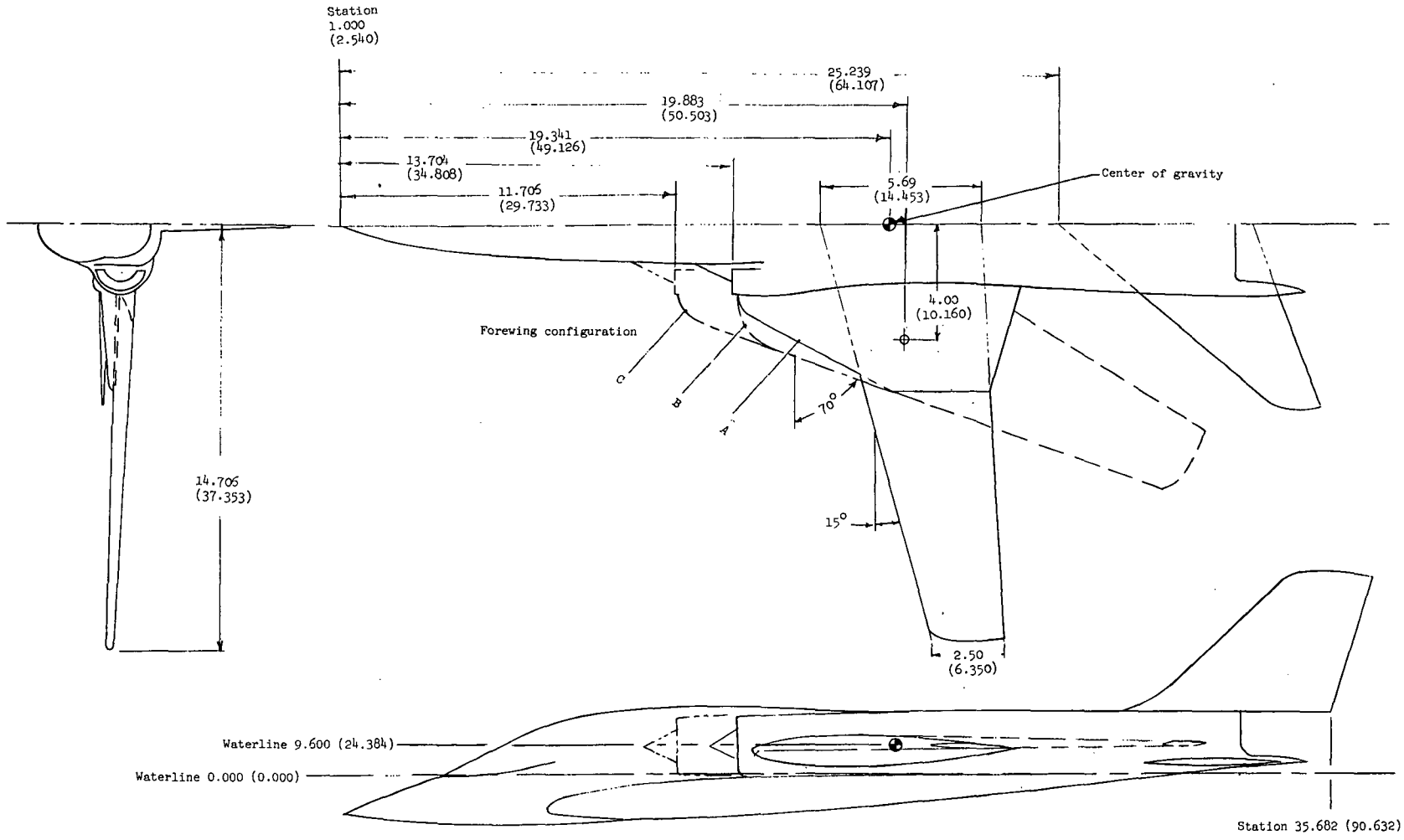

(a) Three-view drawing of model.

Figure 1.- Model details. (All dimensions are given in inches and parenthetically in centimeters unless otherwise noted.)

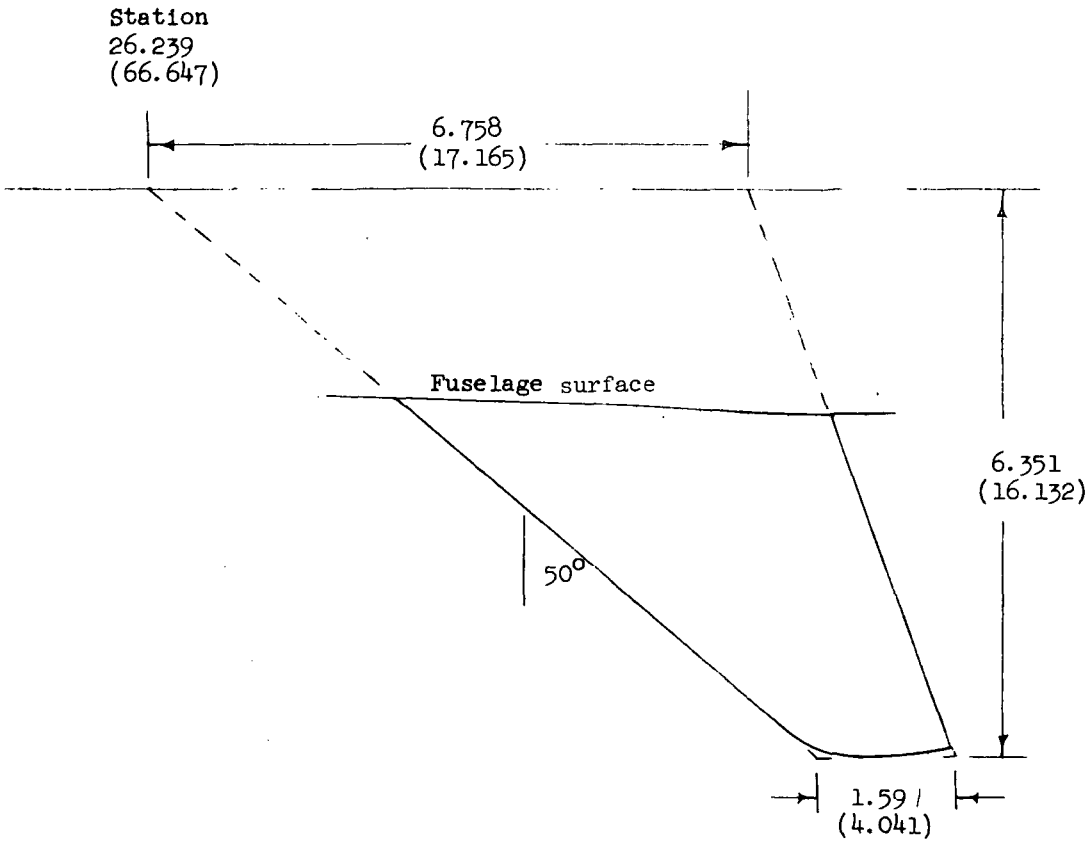

Airfoil section NACA 65A006

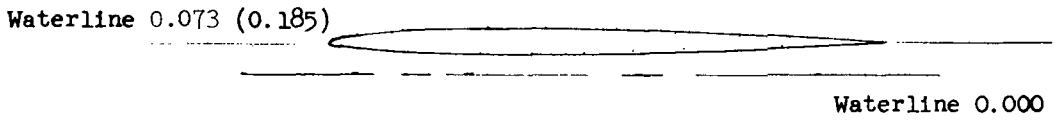

(b) Horizontal tail.

Figure 1.- Continued.

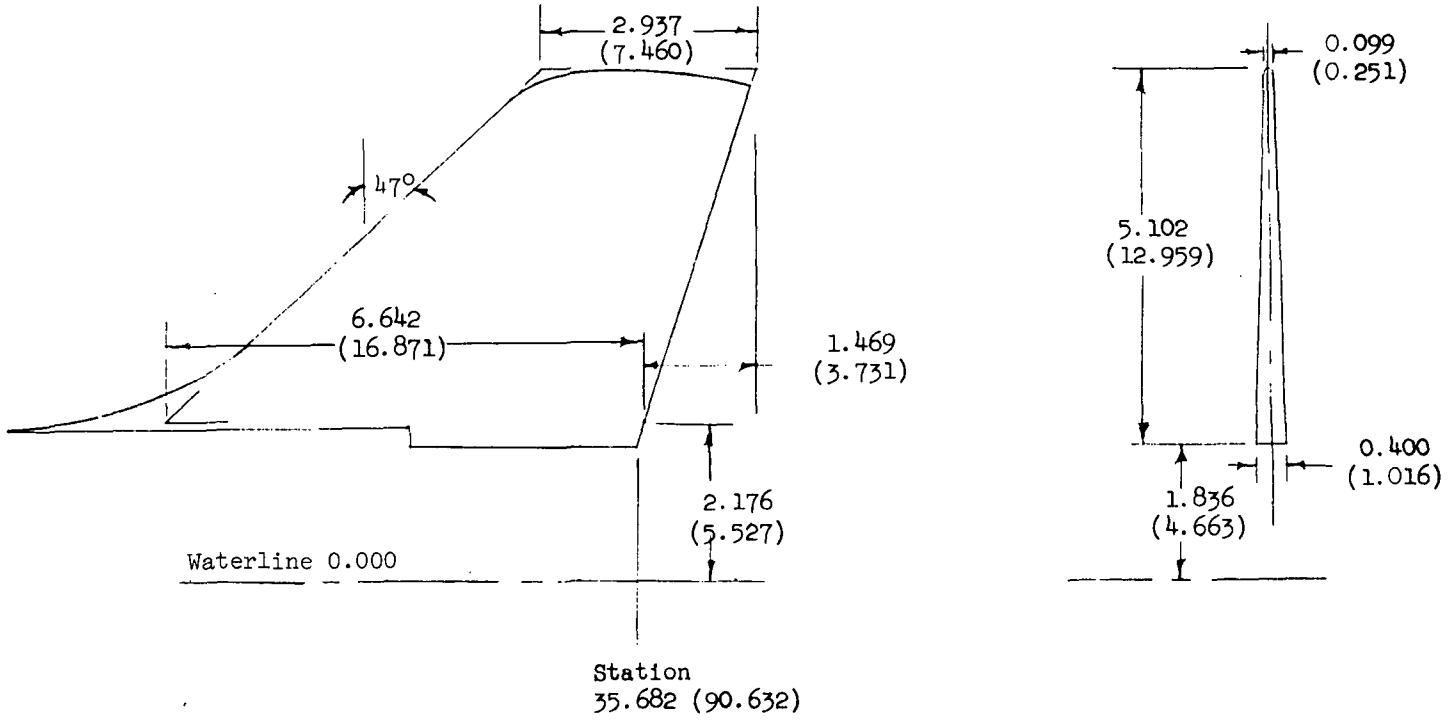

Airfoil section NACA 65A006

(c) Vertical tail.

Figure 1.- Concluded.

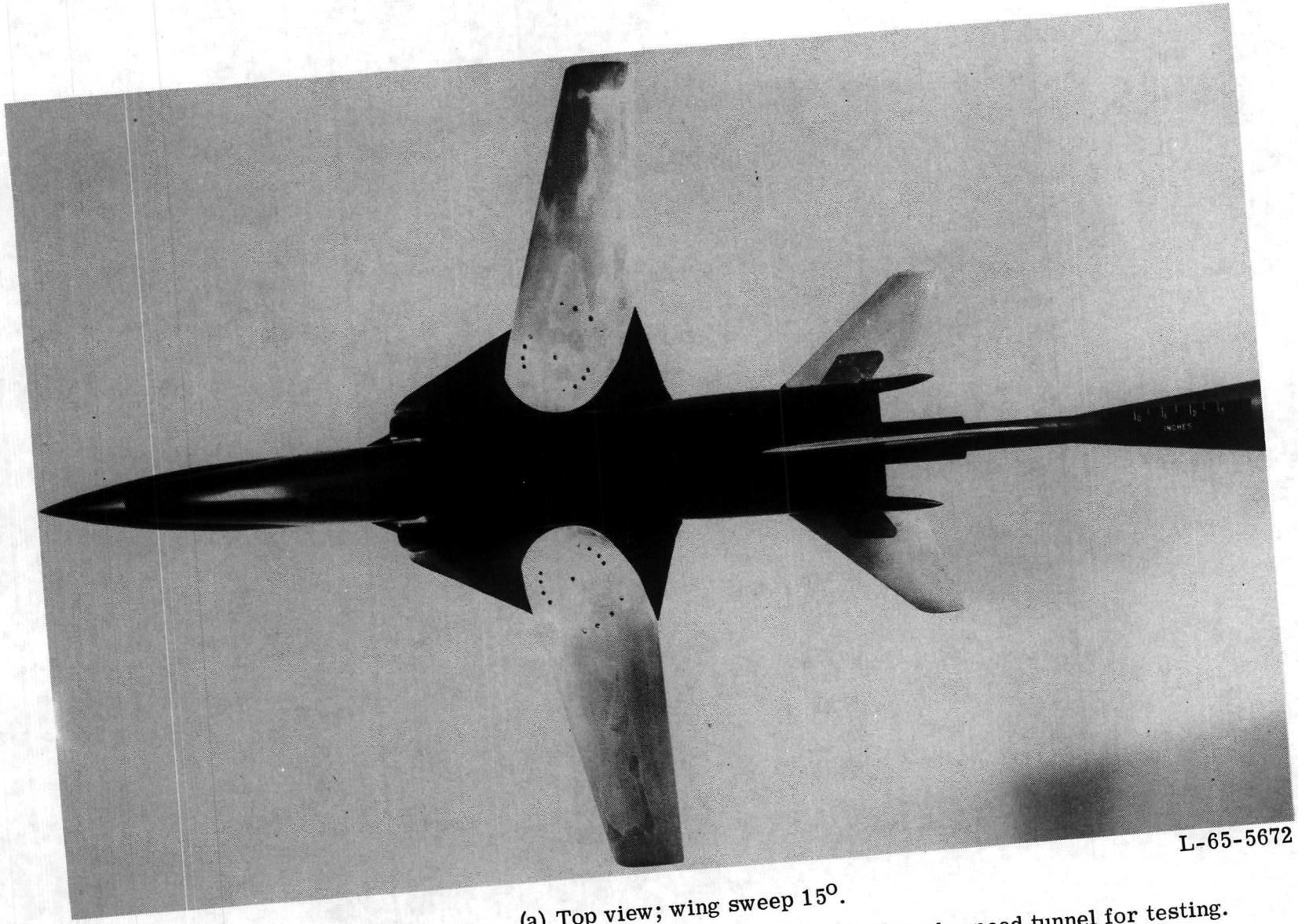

(a) Top view; wing sweep 15°.

Figure 2.- Photographs of model mounted in Langley 7- by 10-foot high-speed tunnel for testing.

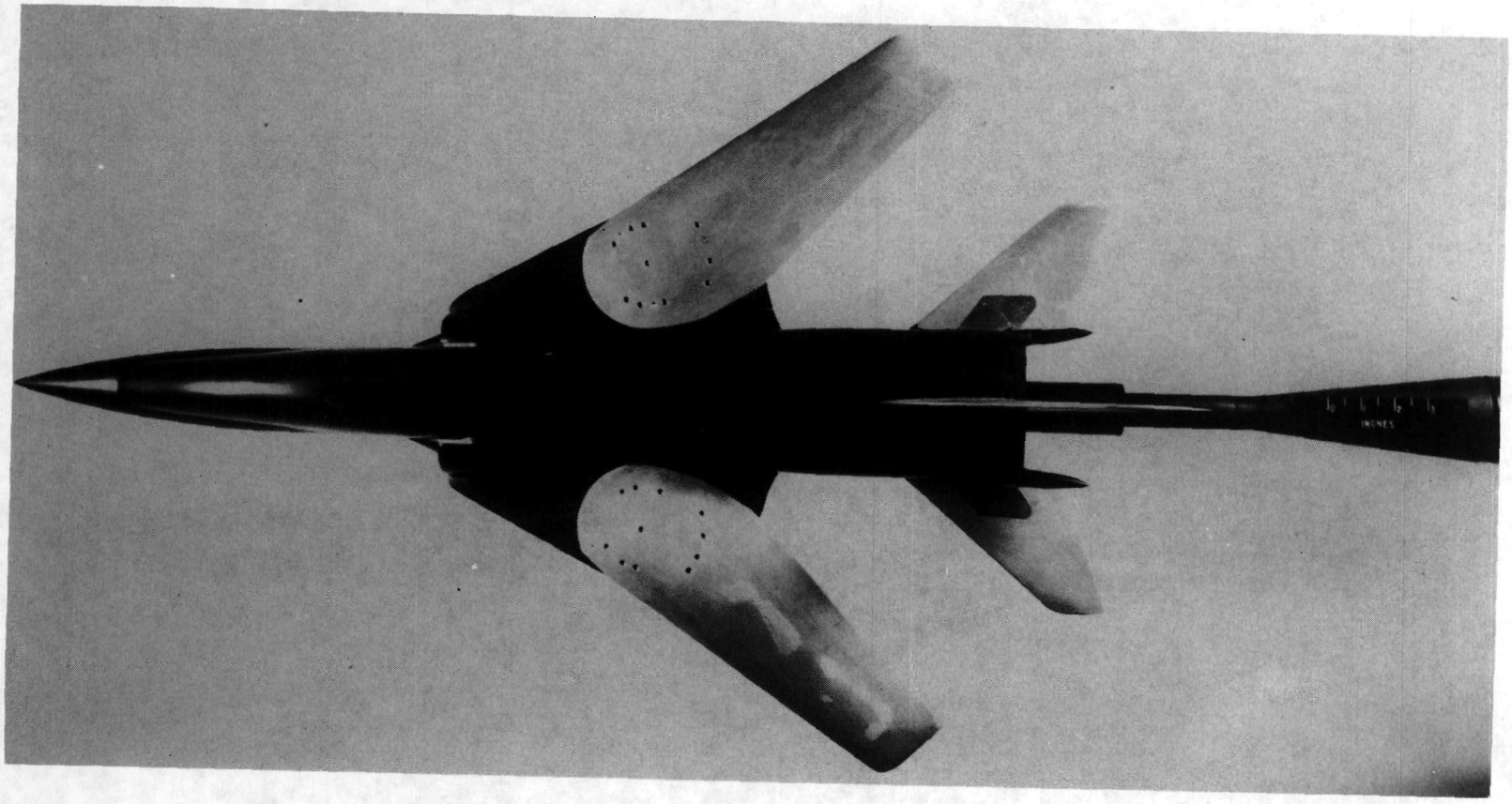

(b) Top view; wing sweep 55°.

L-65-5673

Figure 2.- Continued.

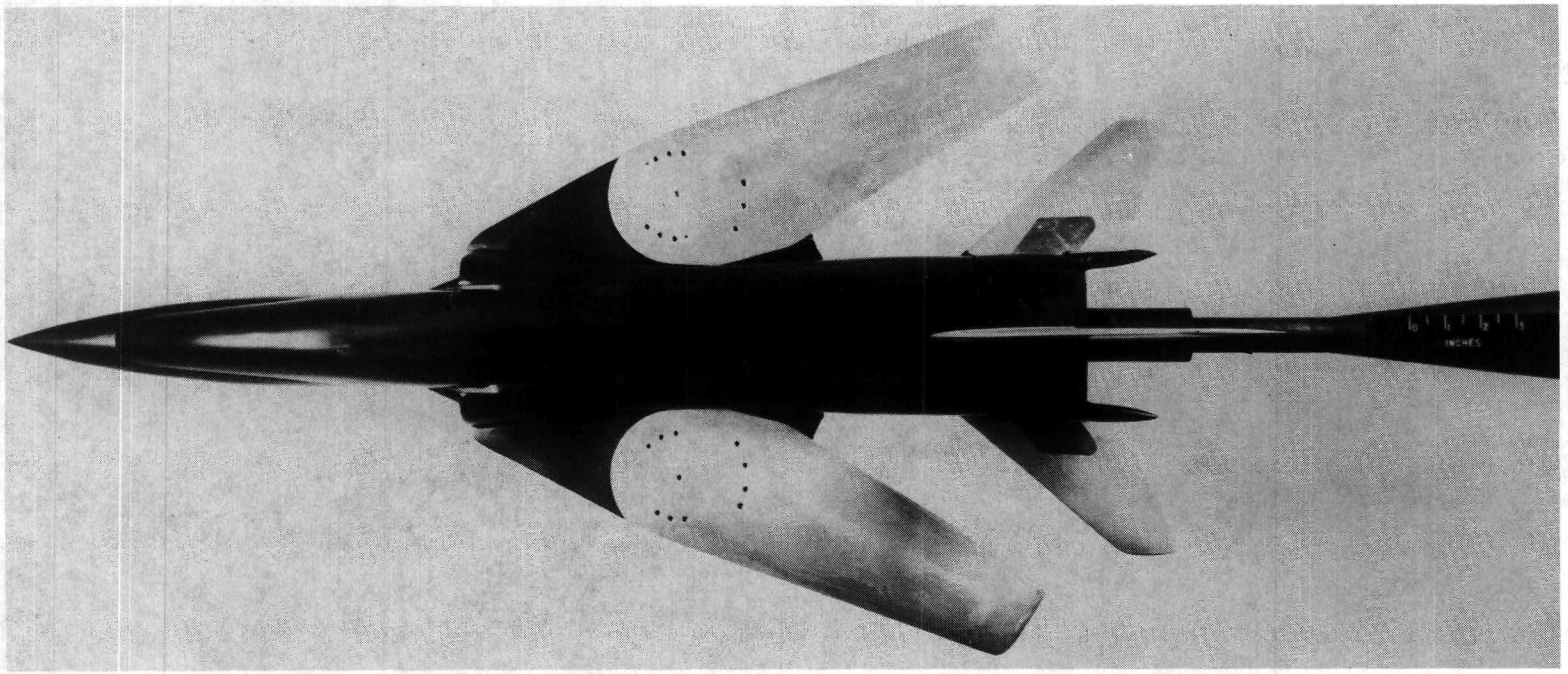

L-65-5671

(c) Top view; wing sweep 70°.

Figure 2.- Continued.

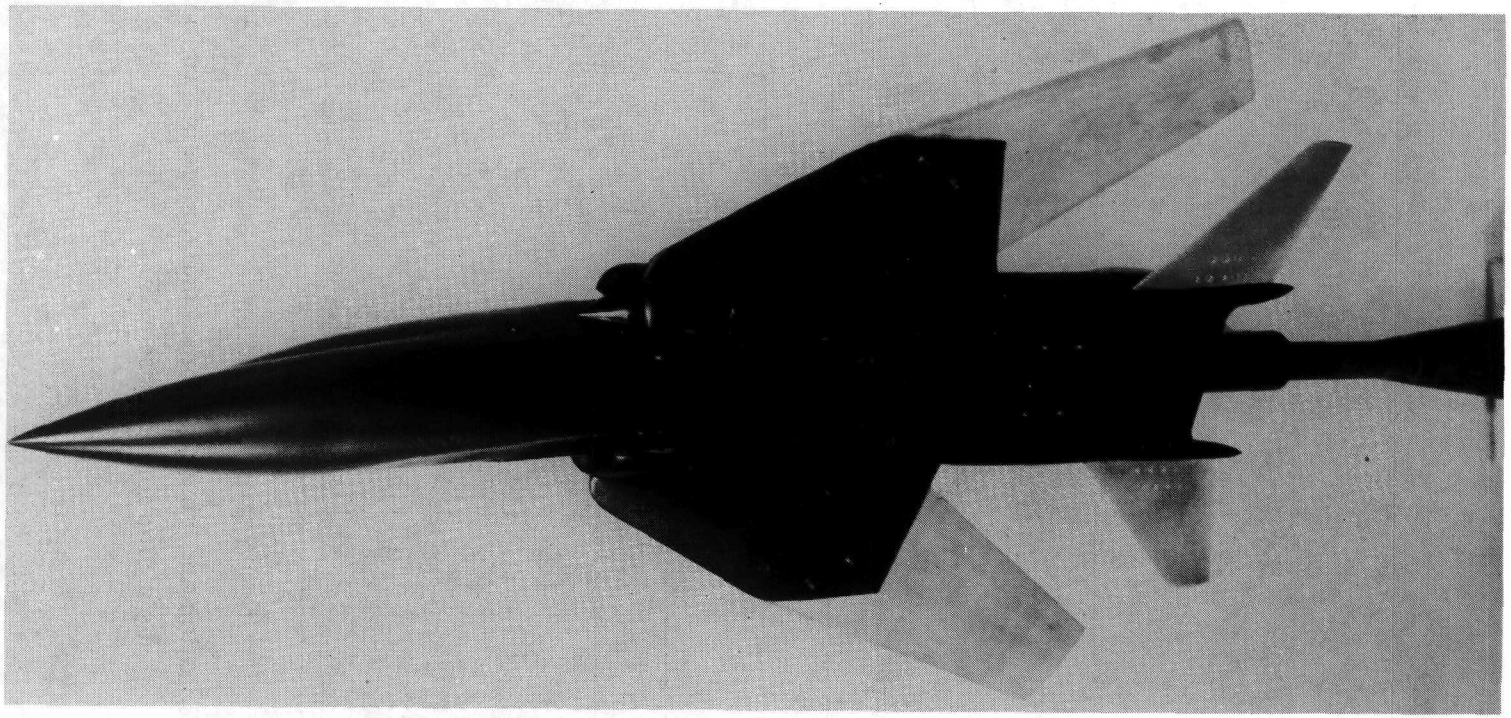

L-65-5676

(d) Three-quarter bottom view; wing sweep 70^{o}.

Figure 2.- Concluded.

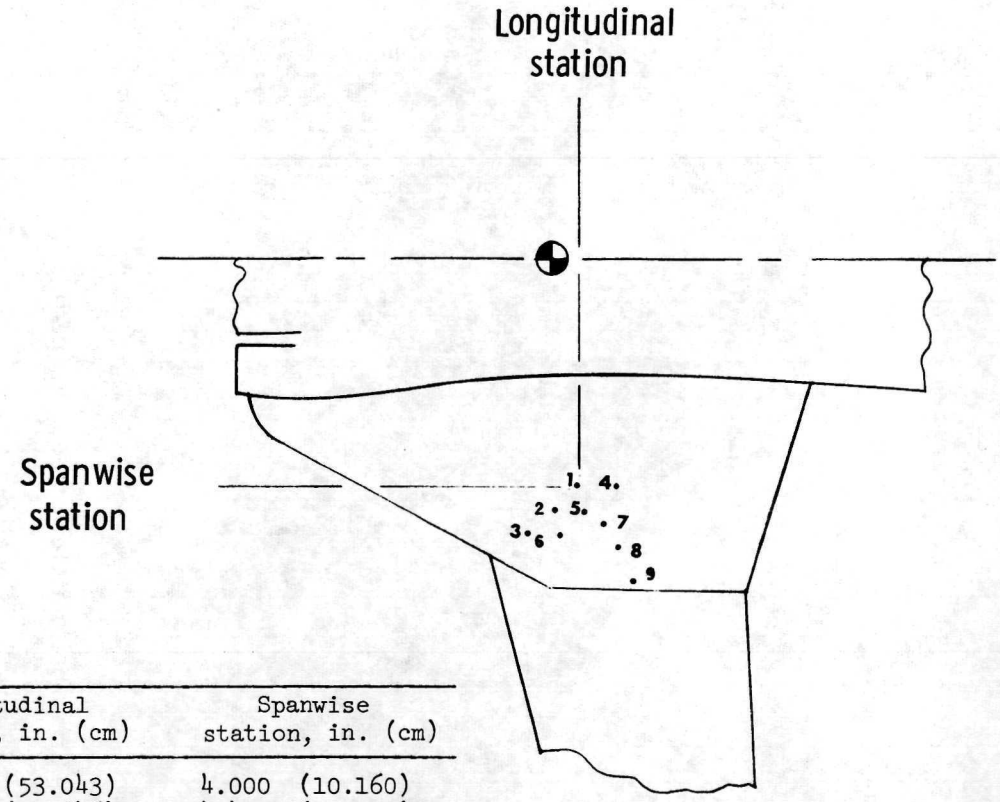

Pivot	Longitudinal station, in. (cm)	Spanwise station, in. (cm)
1	20.883 (53.043)	4.000 (10.160)
2	20.412 (51.846)	4.430 (11.252)
3	20.000 (50.800)	4.805 (12.205)
4	21.435 (54.445)	4.000 (10.160)
5	20.947 (53.205)	4.441 (11.280)
6	20.459 (51.966)	4.882 (12.400)
7	21.312 (54.132)	4.818 (12.238)
8	21.559 (54.760)	5.294 (13.447)
9	21.806 (55.387)	5.770 (14.656)

(a) Wing-pivot location.

Figure 3.- Wing-pivot location and wing position of maximum and minimum sweep as a function of pivot path.

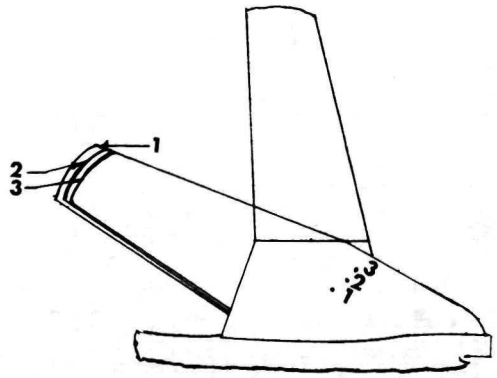

(b) Wing-pivot paths 1, 2, and 3.

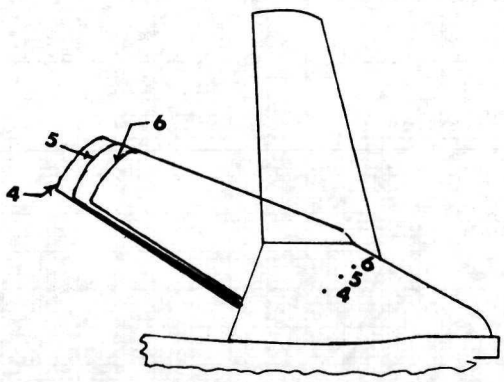

(c) Wing-pivot paths 4, 5, and 6.

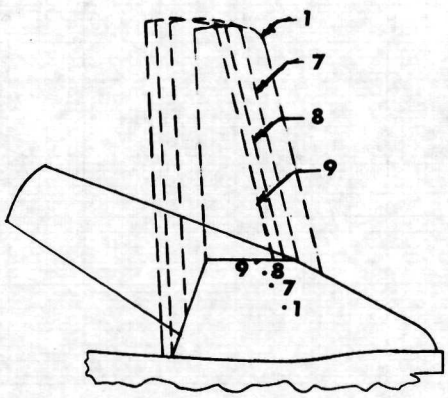

(d) Wing-pivot paths 1, 7, 8, and 9.

Figure 3.- Concluded.

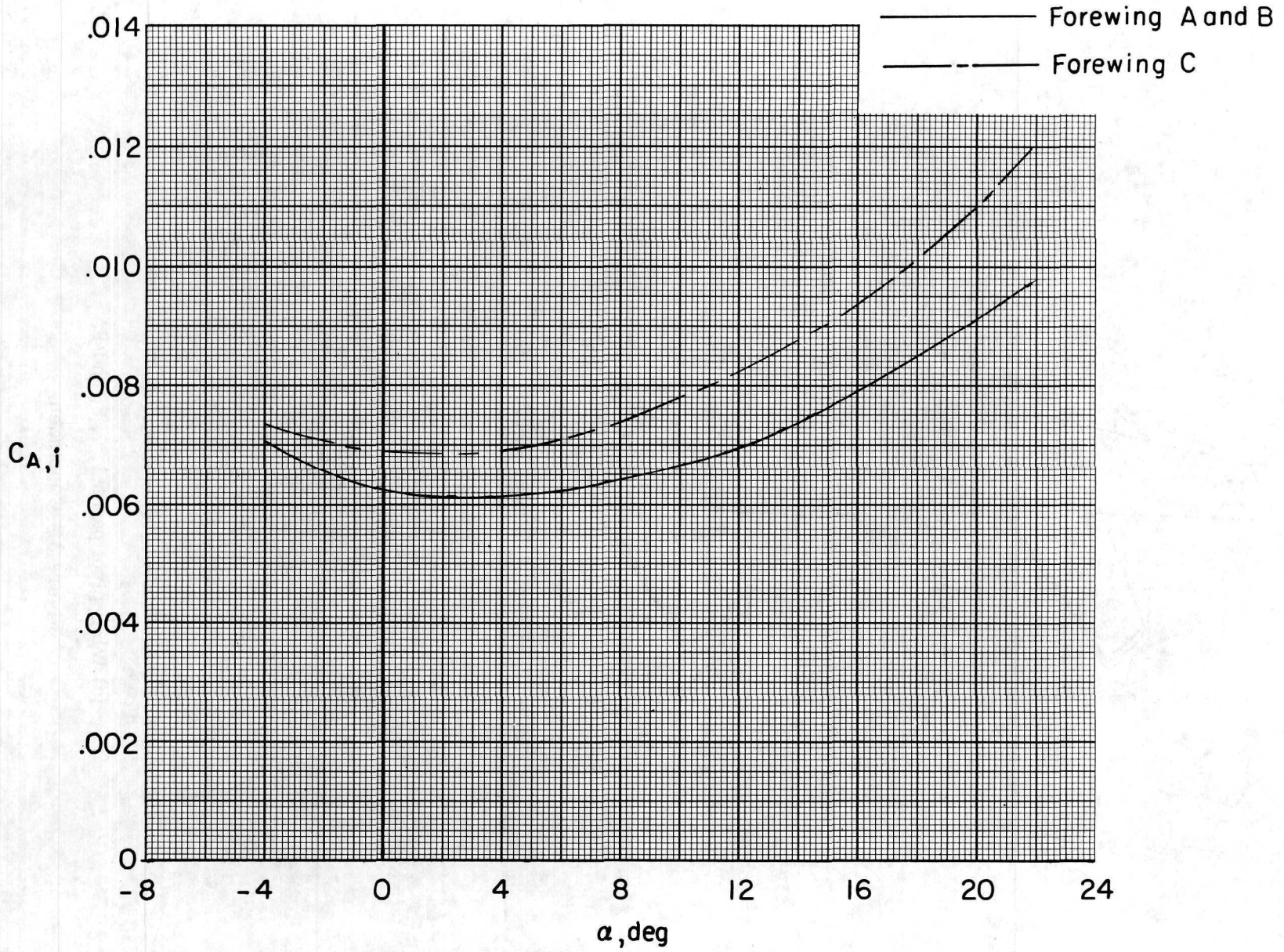

Figure 4.- Variation of internal-flow axial-force corrections with angle of attack.

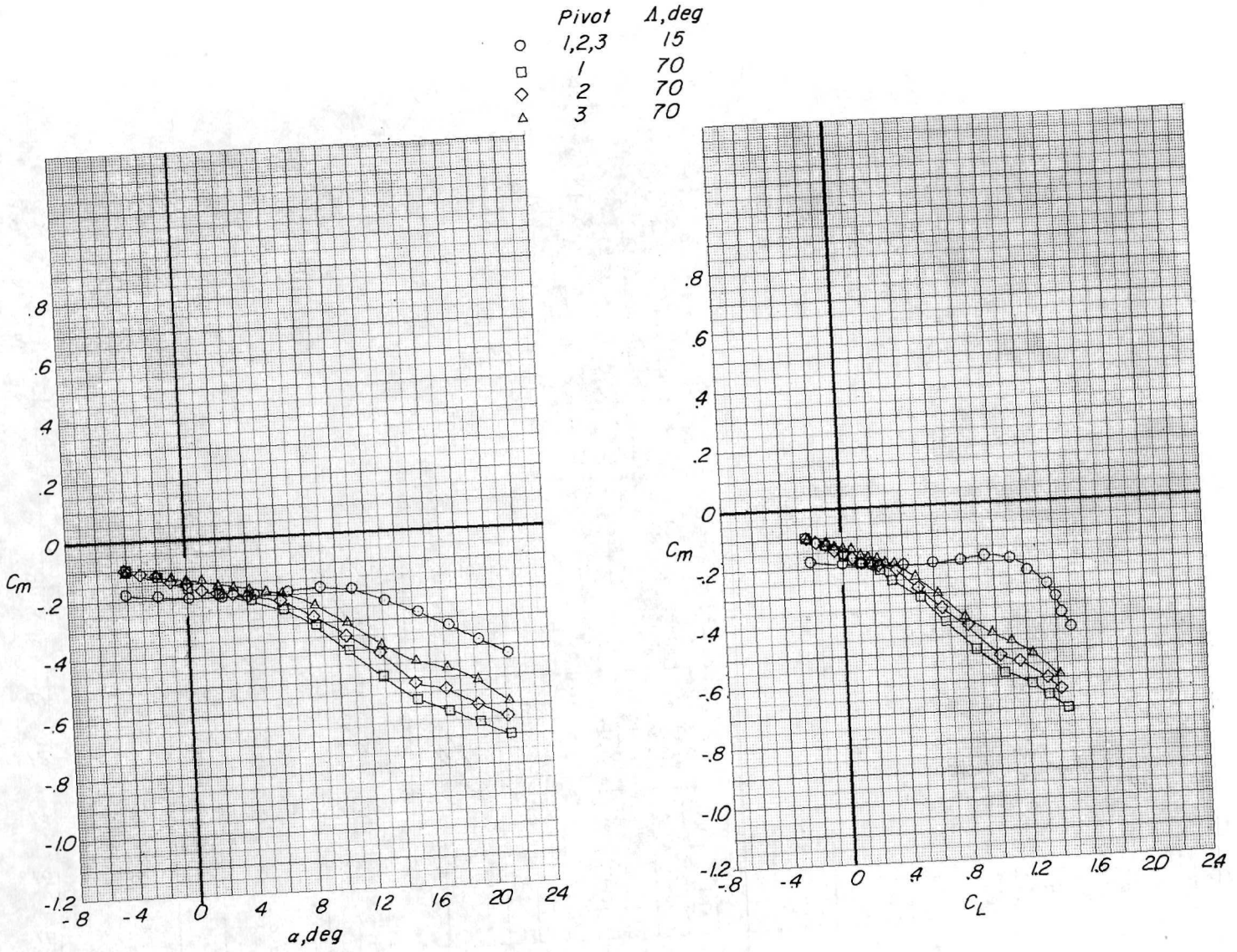

(a) C_m against α and C_L.

Figure 5.- Effect of sweep-angle variation on the aerodynamic characteristics of configurations utilizing pivots 1, 2, and 3. M = 0.27; $i_t = 0^o$; forewing configuration A.

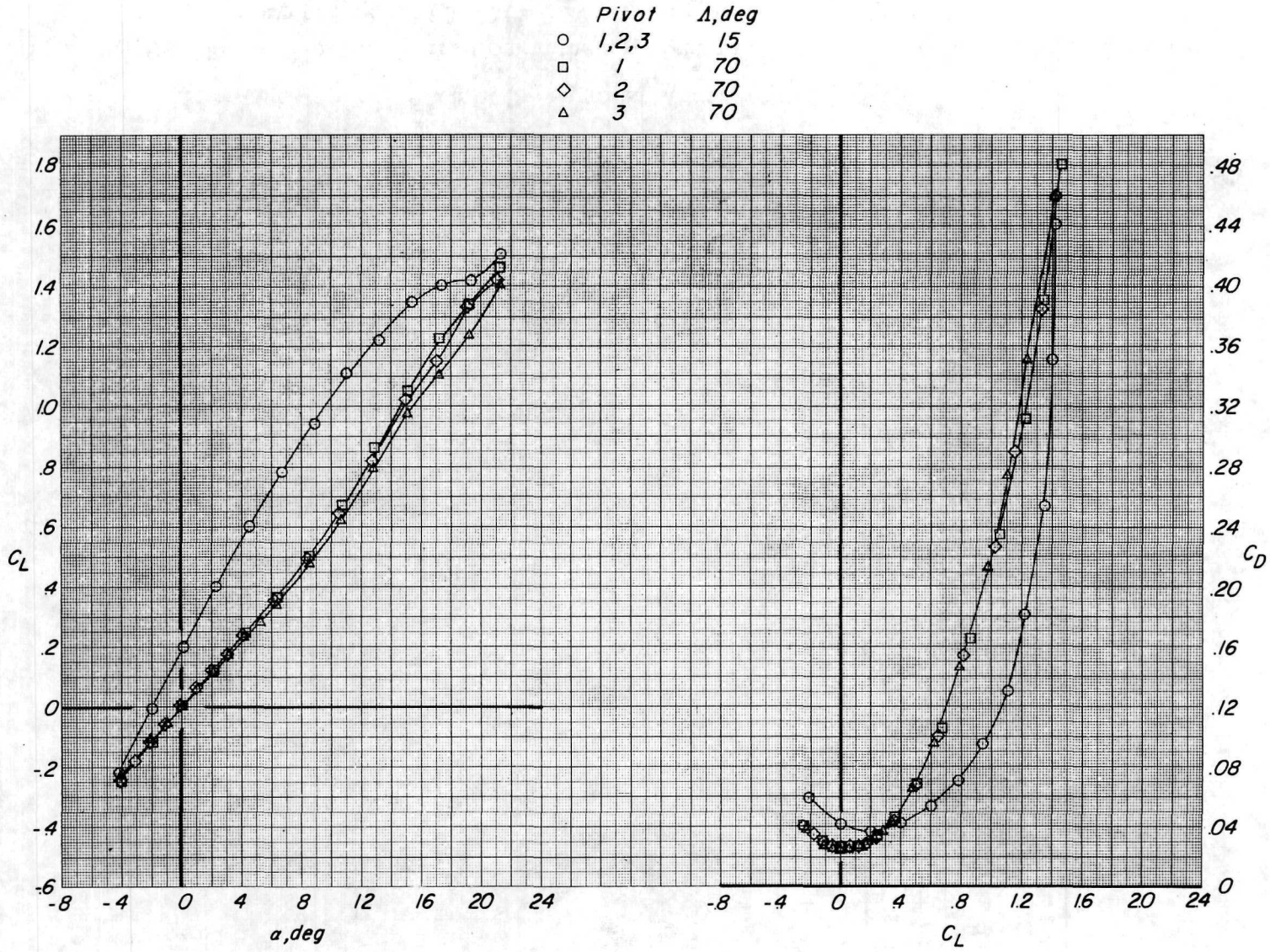

(b) C_L against α and C_D.

Figure 5.- Concluded.

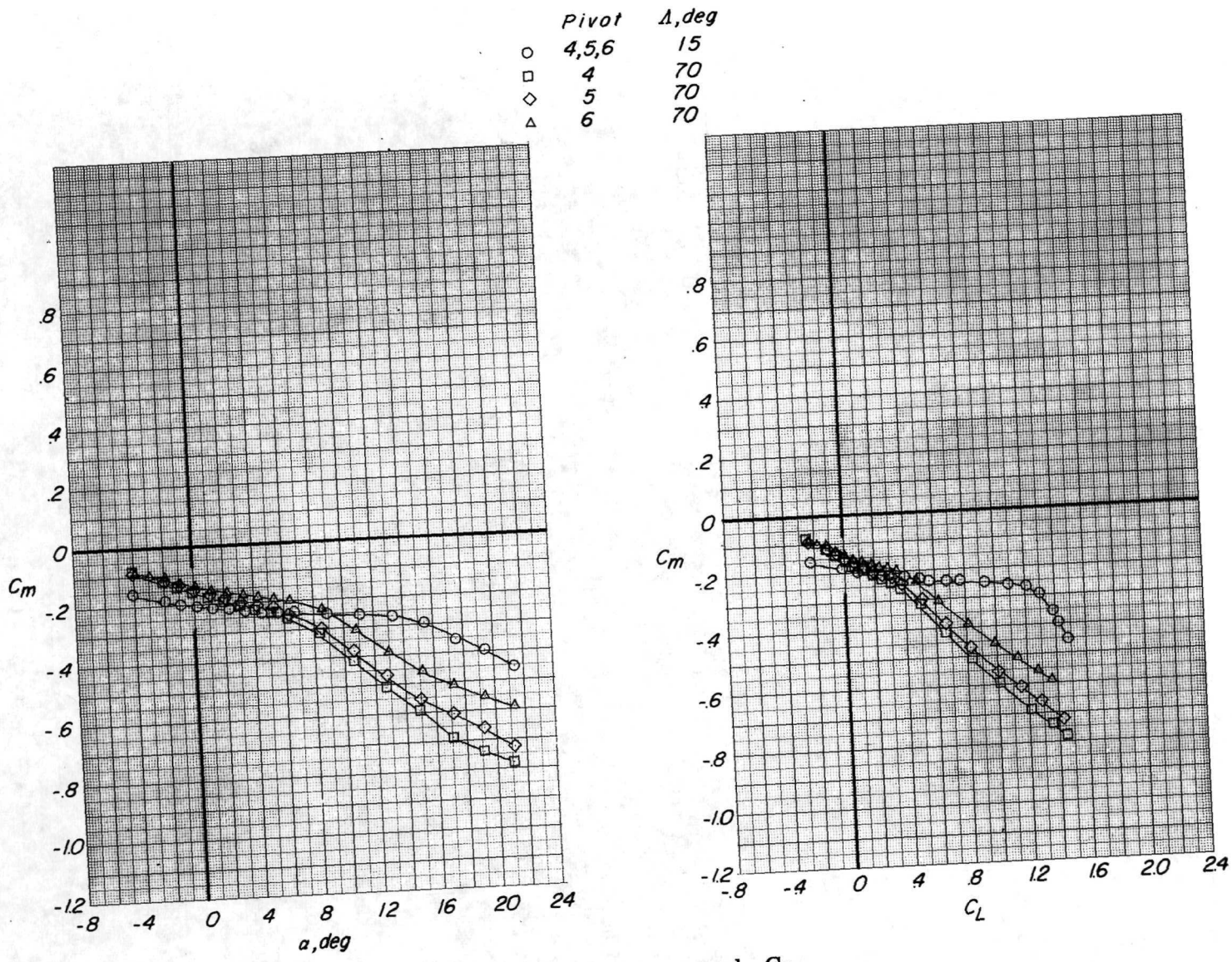

(a) C_m against α and C_L.

Figure 6.- Effect of sweep-angle variation on the aerodynamic characteristics of configurations utilizing pivots 4, 5, and 6. M = 0.27; $i_t = 0^o$; forewing configuration A.

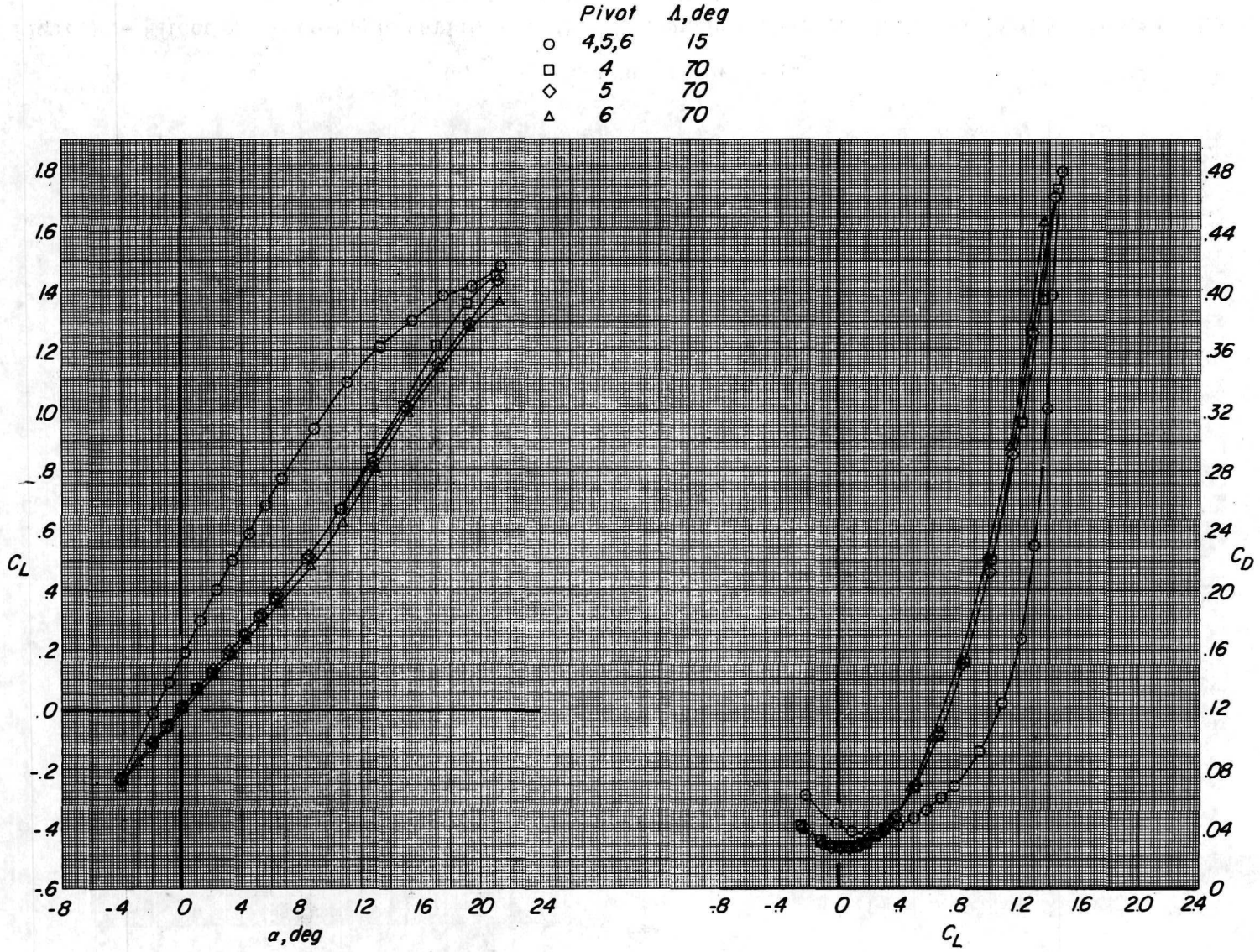

(b) C_L against α and C_D.

Figure 6.- Concluded.

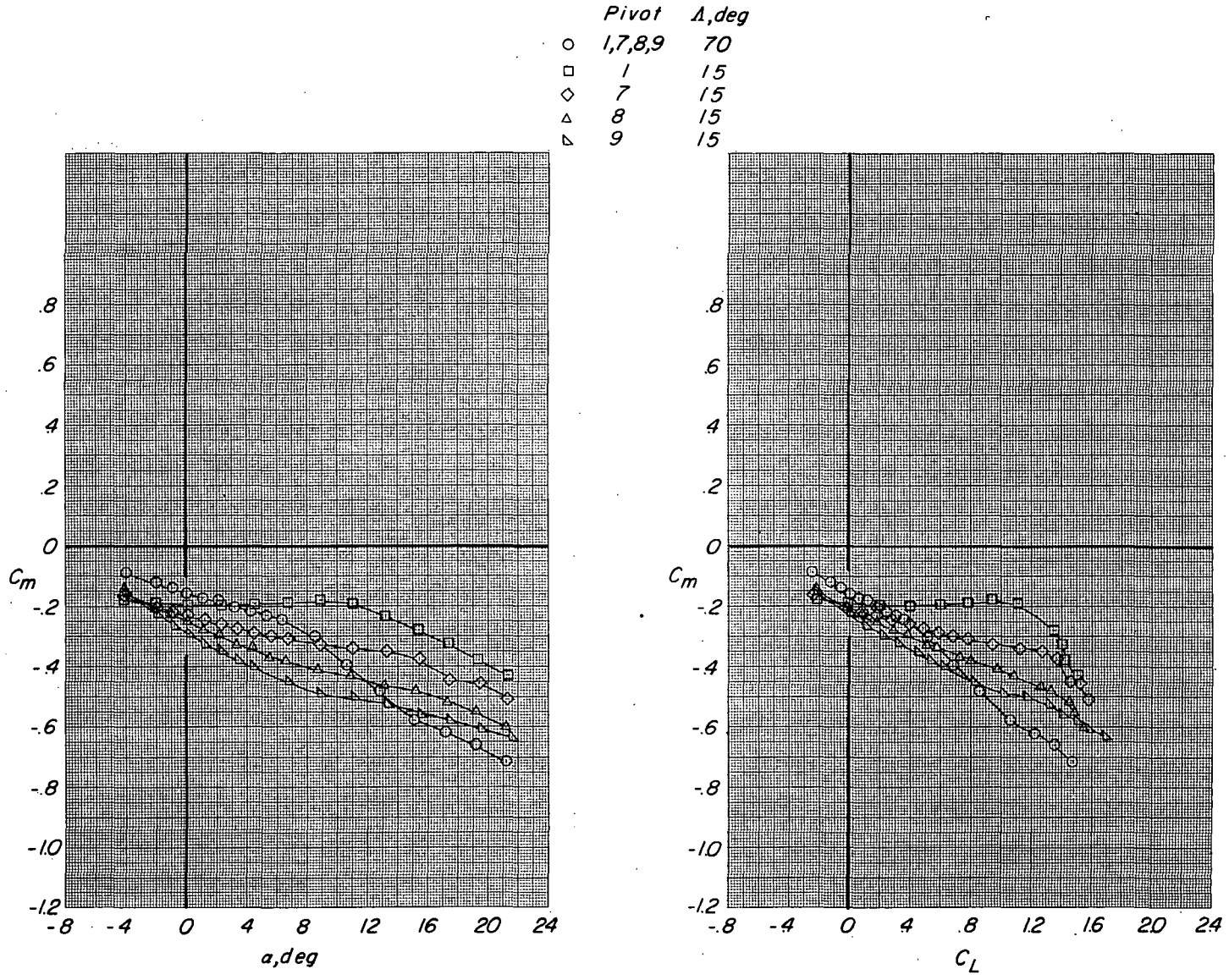

(a) C_m against α and C_L.

Figure 7.- Effect of sweep-angle variation on the aerodynamic characteristics of configurations utilizing pivots 1, 7, 8, and 9. M = 0.27; $i_t = 0^o$; forewing configuration A.

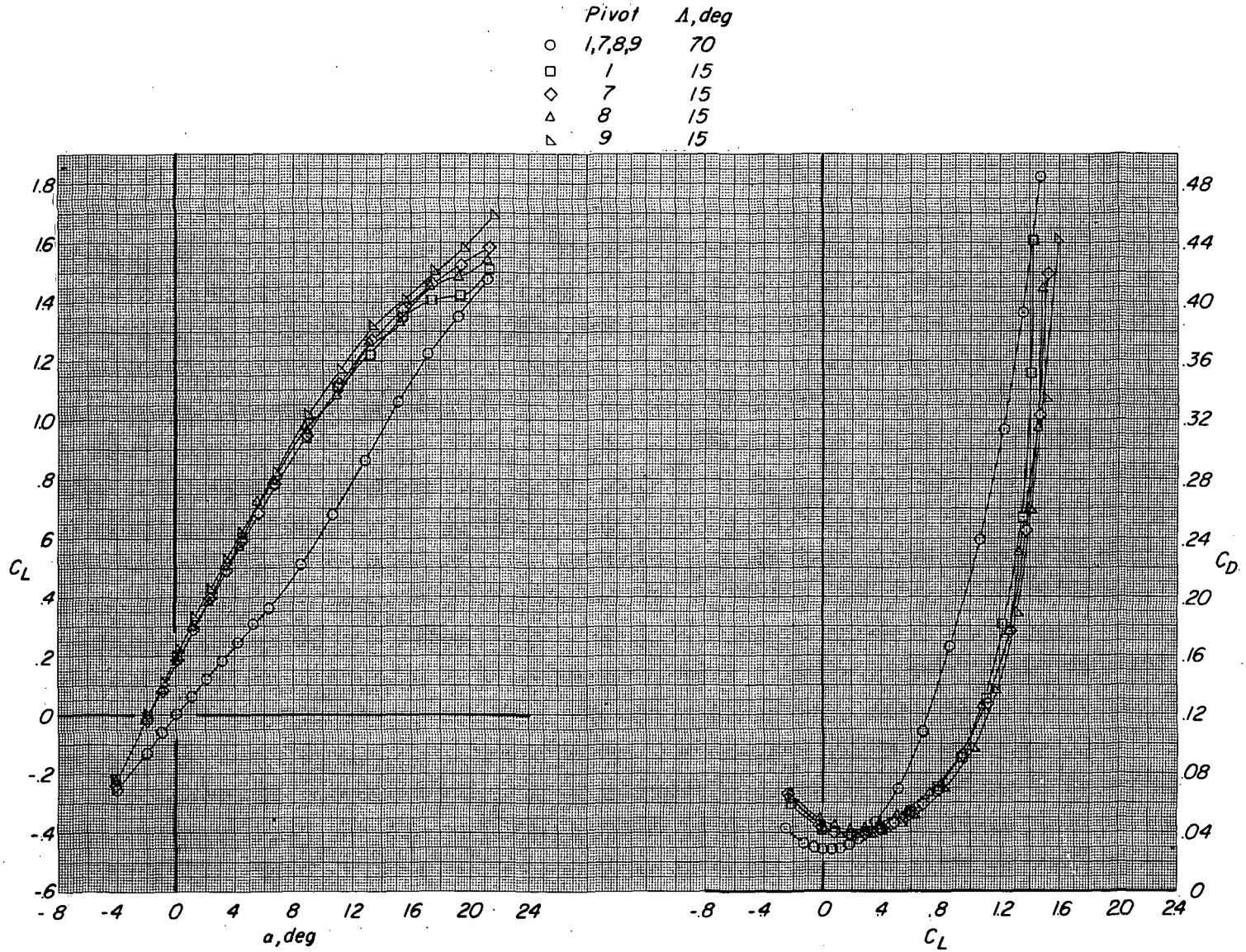

(b) C_L against α and C_D.

Figure 7.- Concluded.

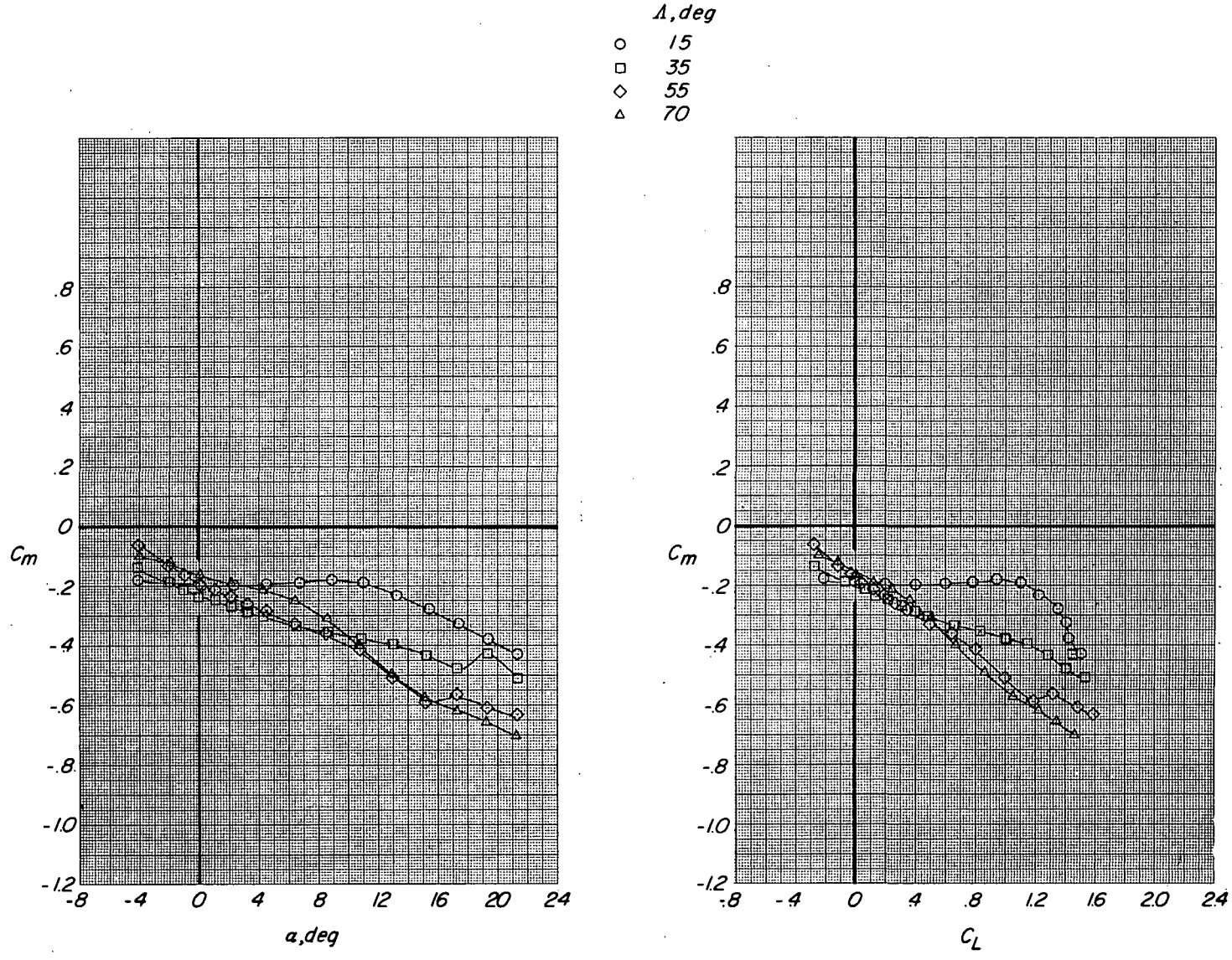

(a) C_m against α and C_L.

Figure 8.- Effect of sweep-angle variation on the aerodynamic characteristics of configuration utilizing pivot 1. M = 0.27; $i_t = 0^o$; forewing configuration A.

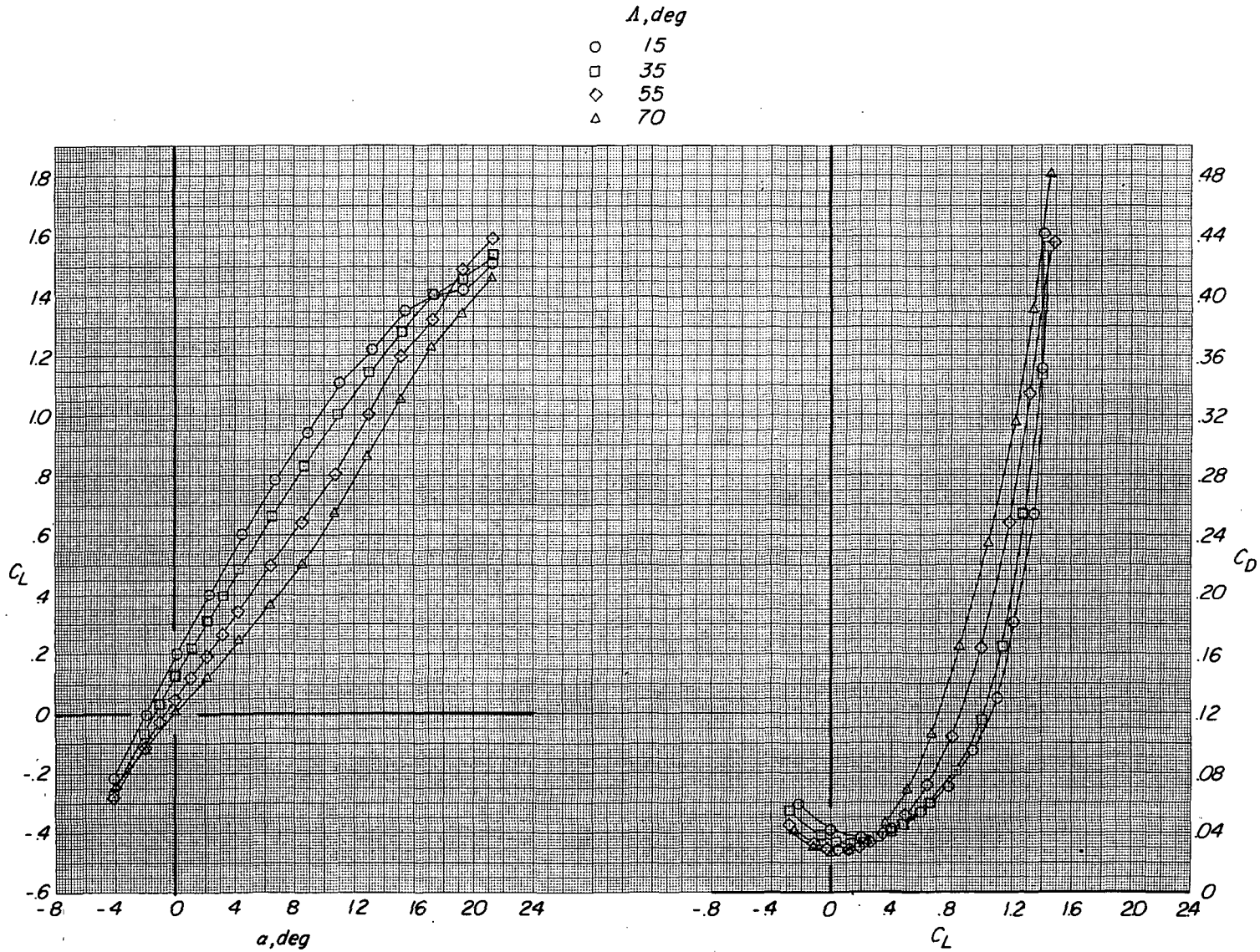

(b) C_L against α and C_D.

Figure 8.- Concluded.

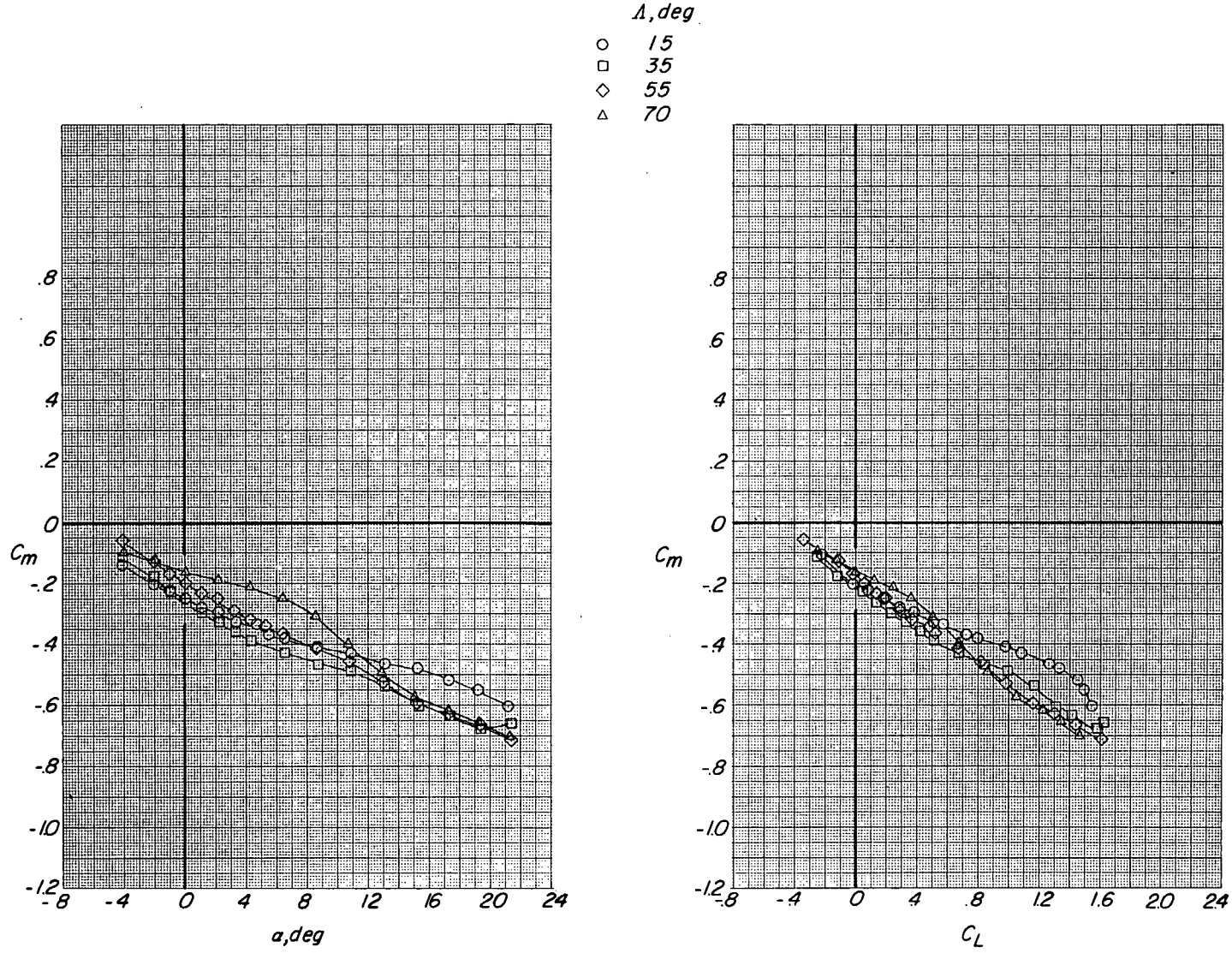

(a) C_m against α and C_L.

Figure 9.- Effect of sweep-angle variation on the aerodynamic characteristics of configuration utilizing pivot 8. M = 0.27; $i_t = 0^o$; forewing configuration A.

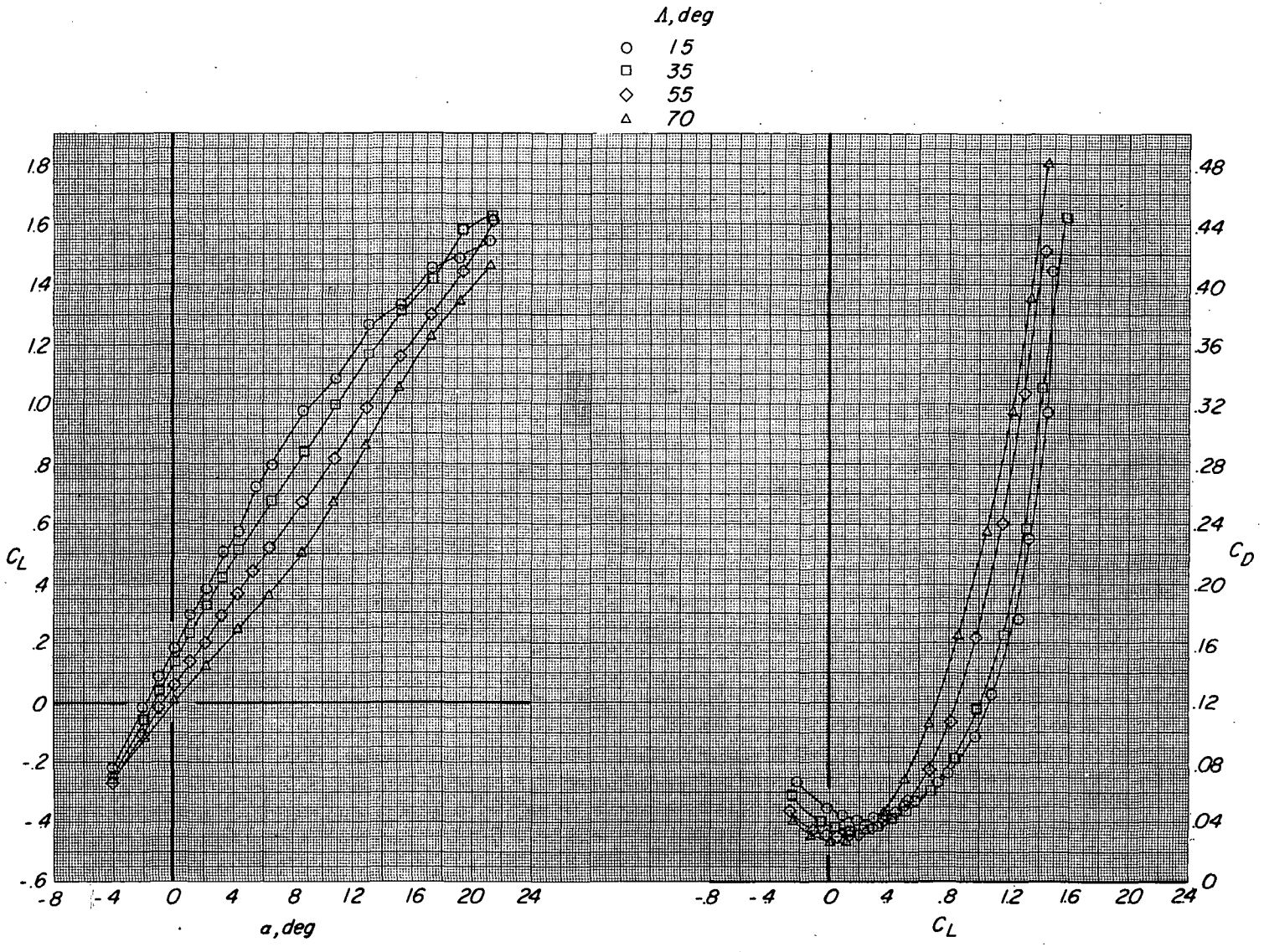

(b) C_L against α and C_D.

Figure 9.- Concluded.

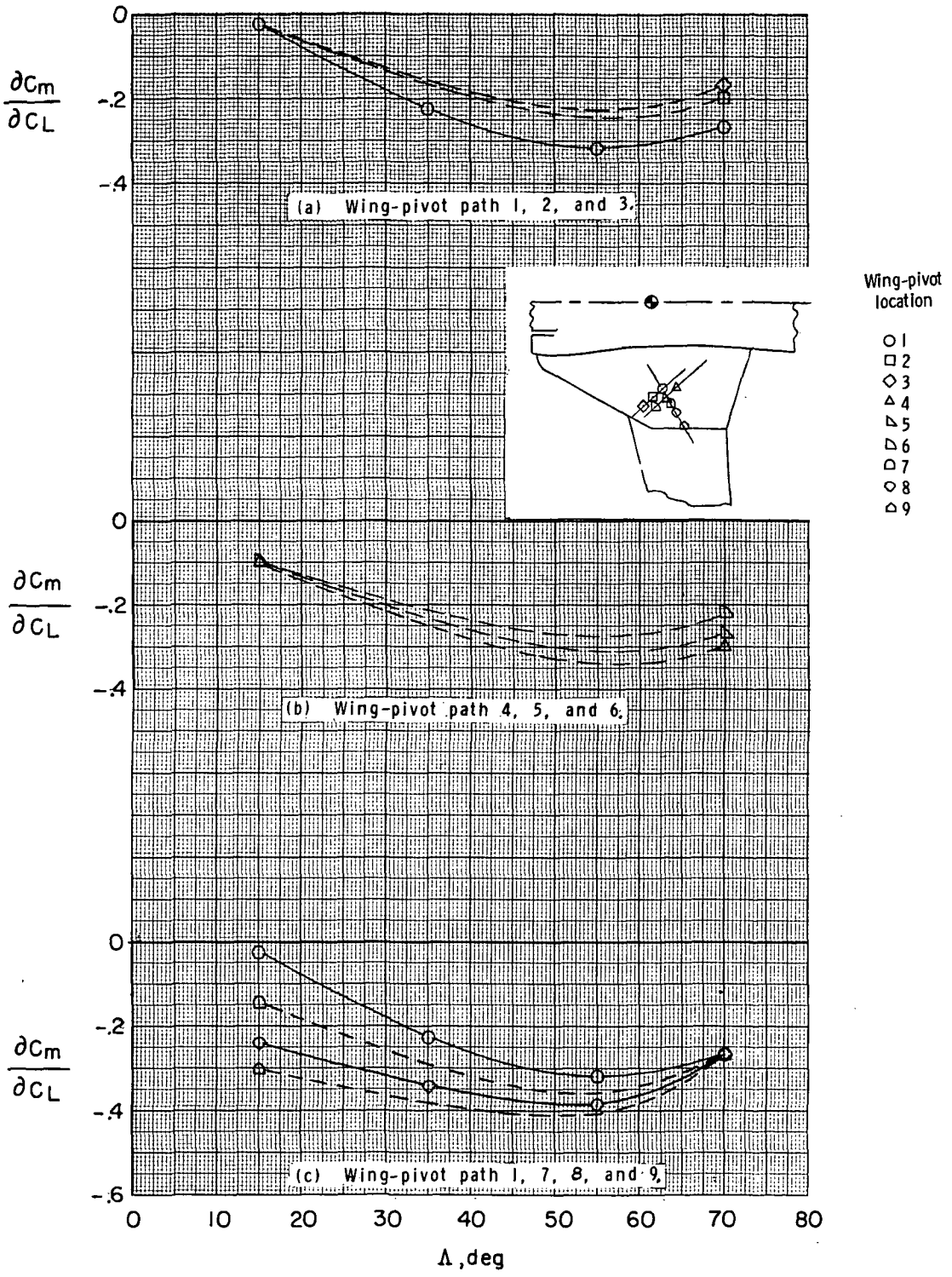

Figure 10.- Variation of static margin as a function of wing sweep angle for the three wing-pivot paths. M = 0.27; forewing configuration A.

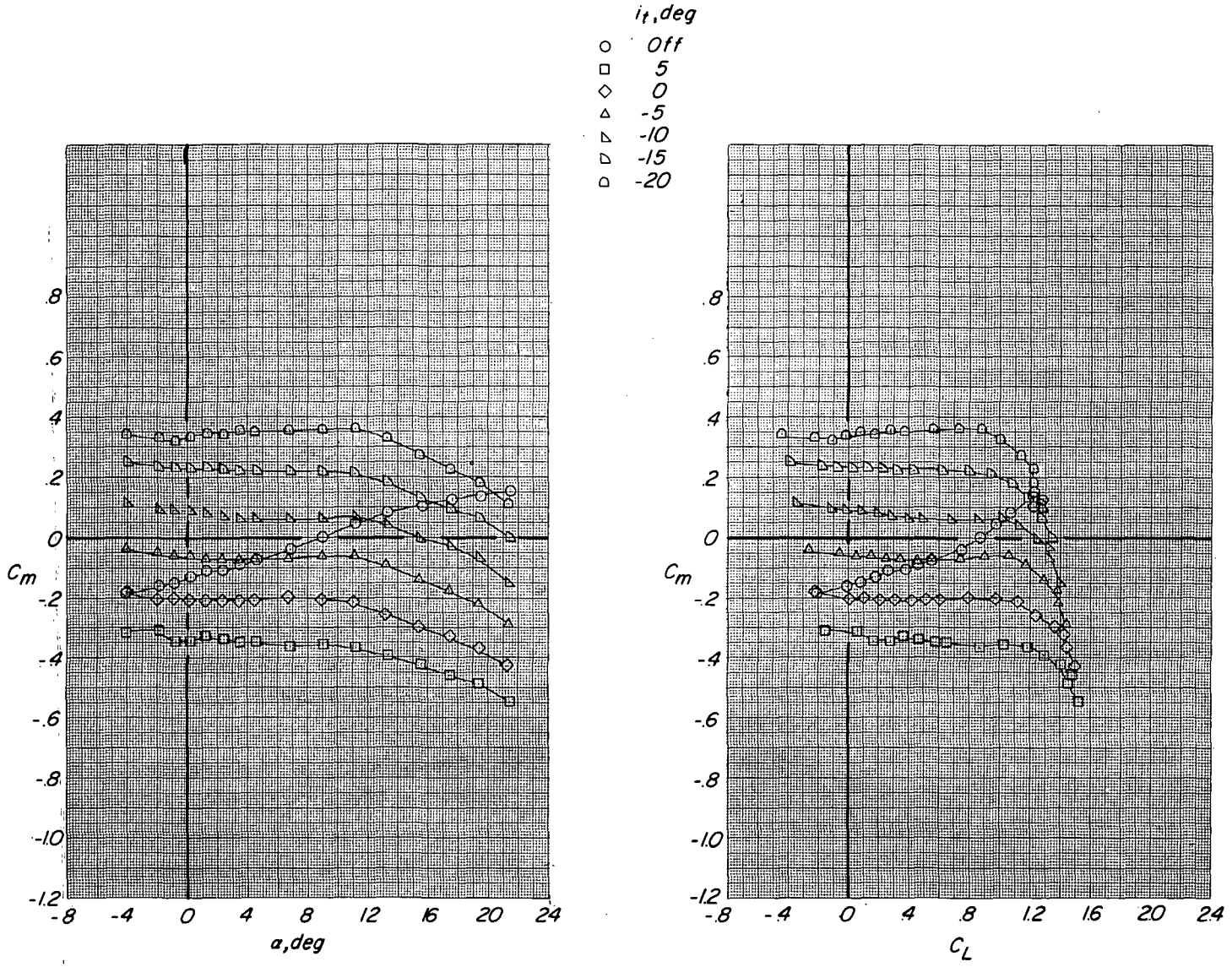

(a) C_m against α and C_L.

Figure 11.- Effect of tail-incidence variation on the aerodynamic characteristics of configuration utilizing pivot 1. $M = 0.27$; $\Lambda = 15^{\circ}$; forewing configuration A.

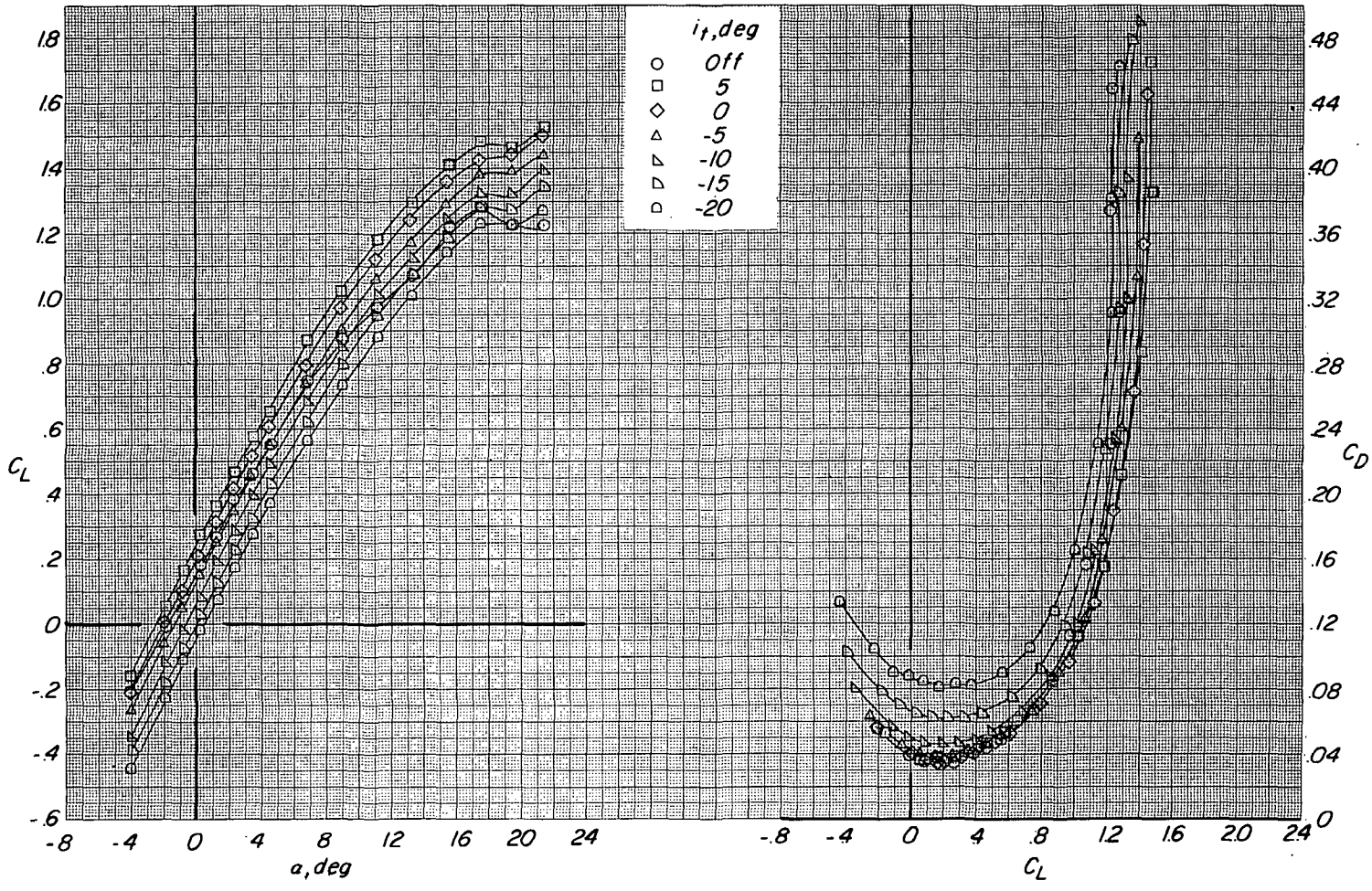

(b) C_L against α and C_D.

Figure 11.- Concluded.

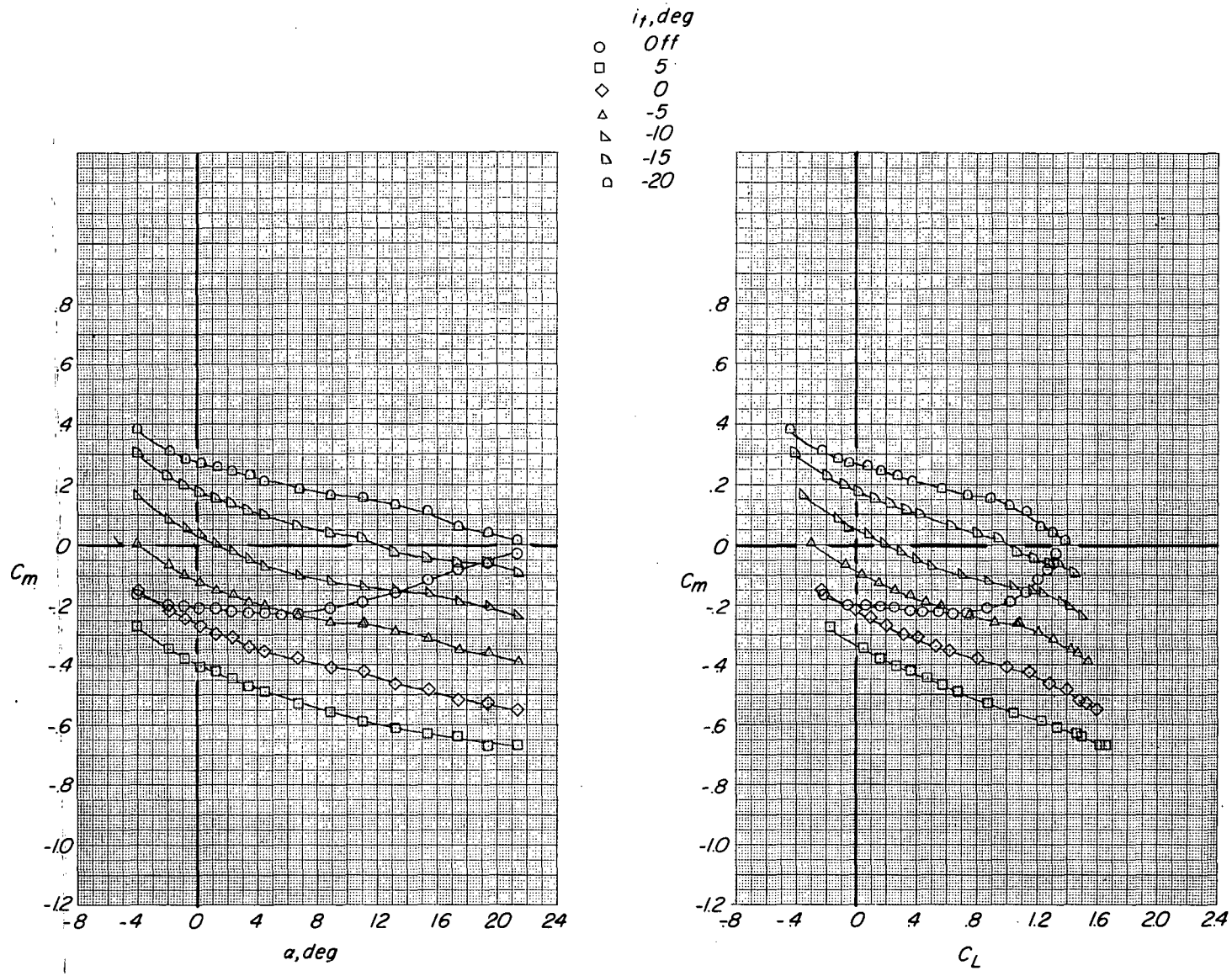

(a) C_m against α and C_L.

Figure 12.- Effect of tail-incidence variation on the aerodynamic characteristics of configuration utilizing pivot 8. M = 0.27; $\Lambda = 15^{\circ}$; forewing configuration A.

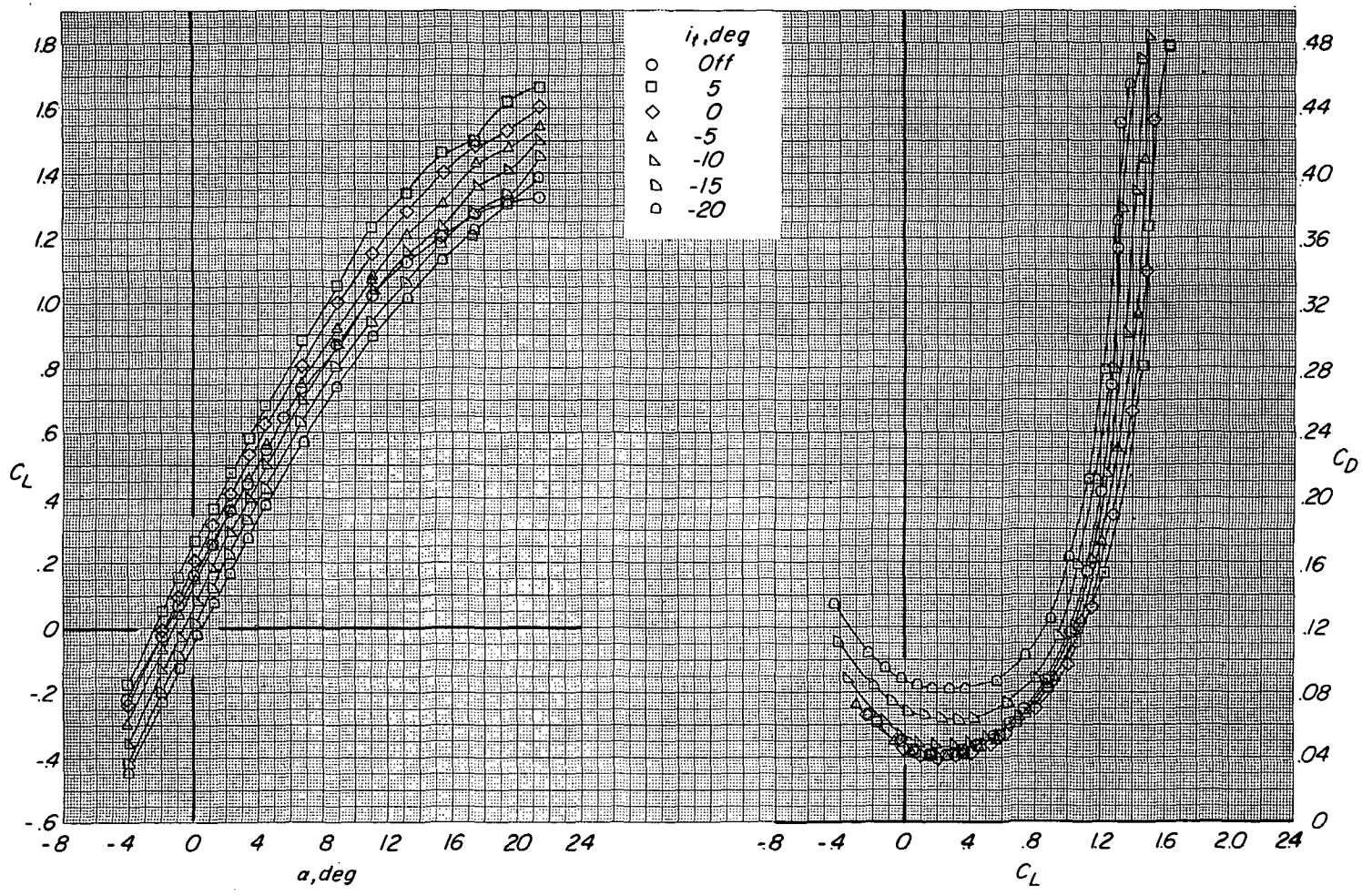

(b) C_L against α and C_D.

Figure 12.- Concluded.

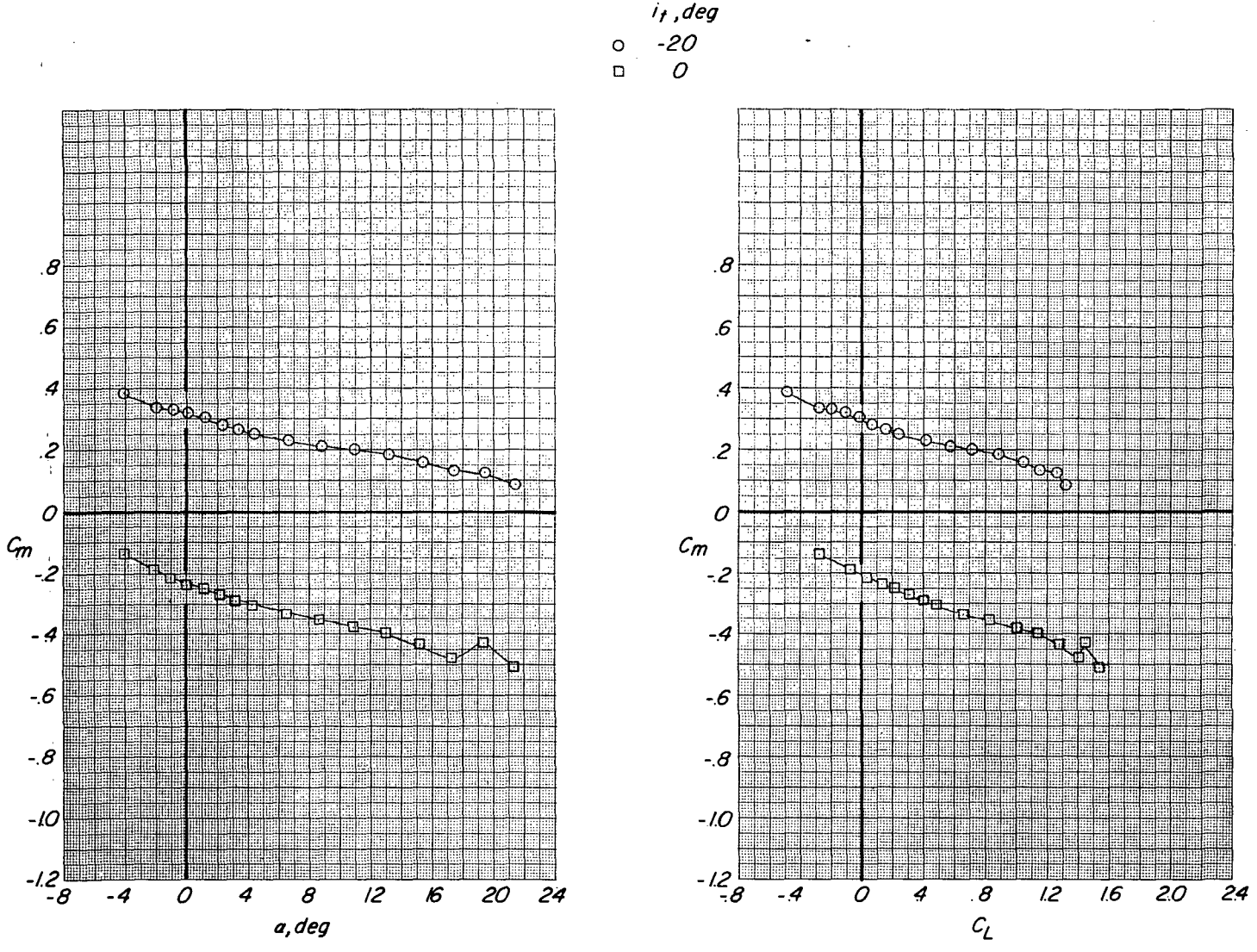

(a) C_m against α and C_L.

Figure 13.- Effect of tail-incidence variation on the aerodynamic characteristics of configuration utilizing pivot 1. M = 0.27; $\Lambda = 35^{o}$; forewing configuration A.

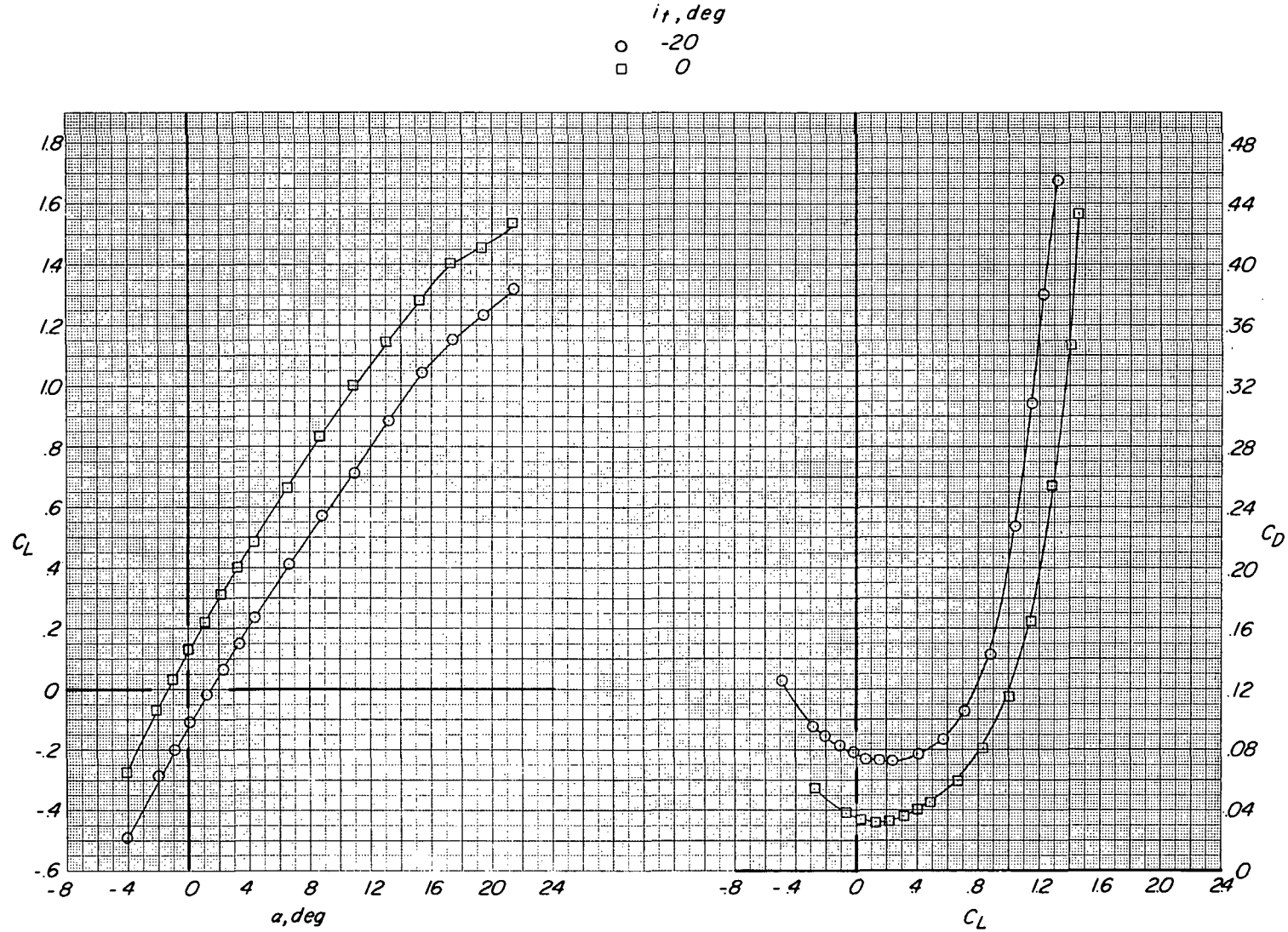

(b) C_L against α and C_D.

Figure 13.- Concluded.

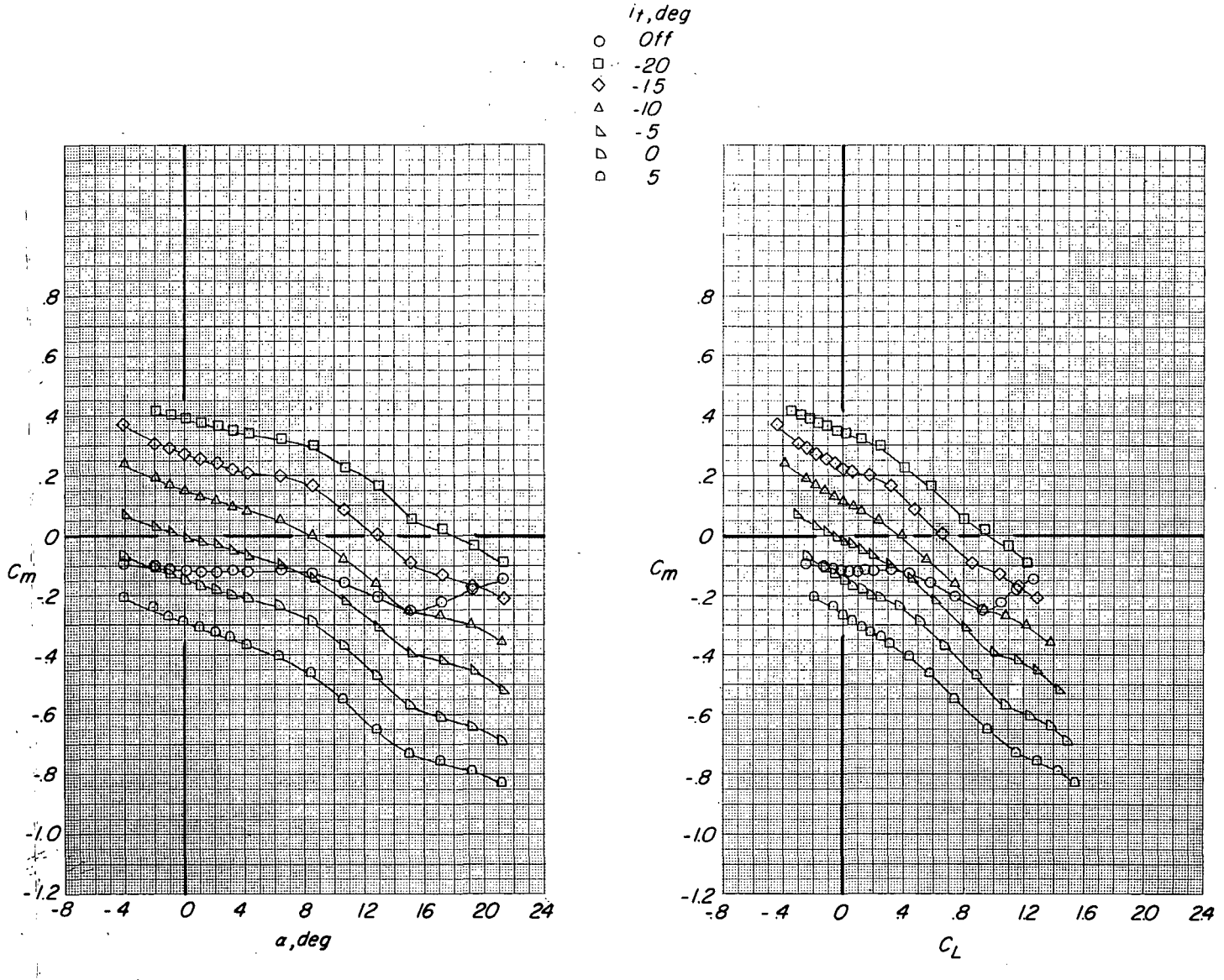

(a) C_m against α and C_L.

Figure 14.- Effect of tail-incidence variation on the aerodynamic characteristics of configurations utilizing pivots 1, 7, 8, and 9. M = 0.27; $\Lambda = 70^{\circ}$; forewing configuration A.

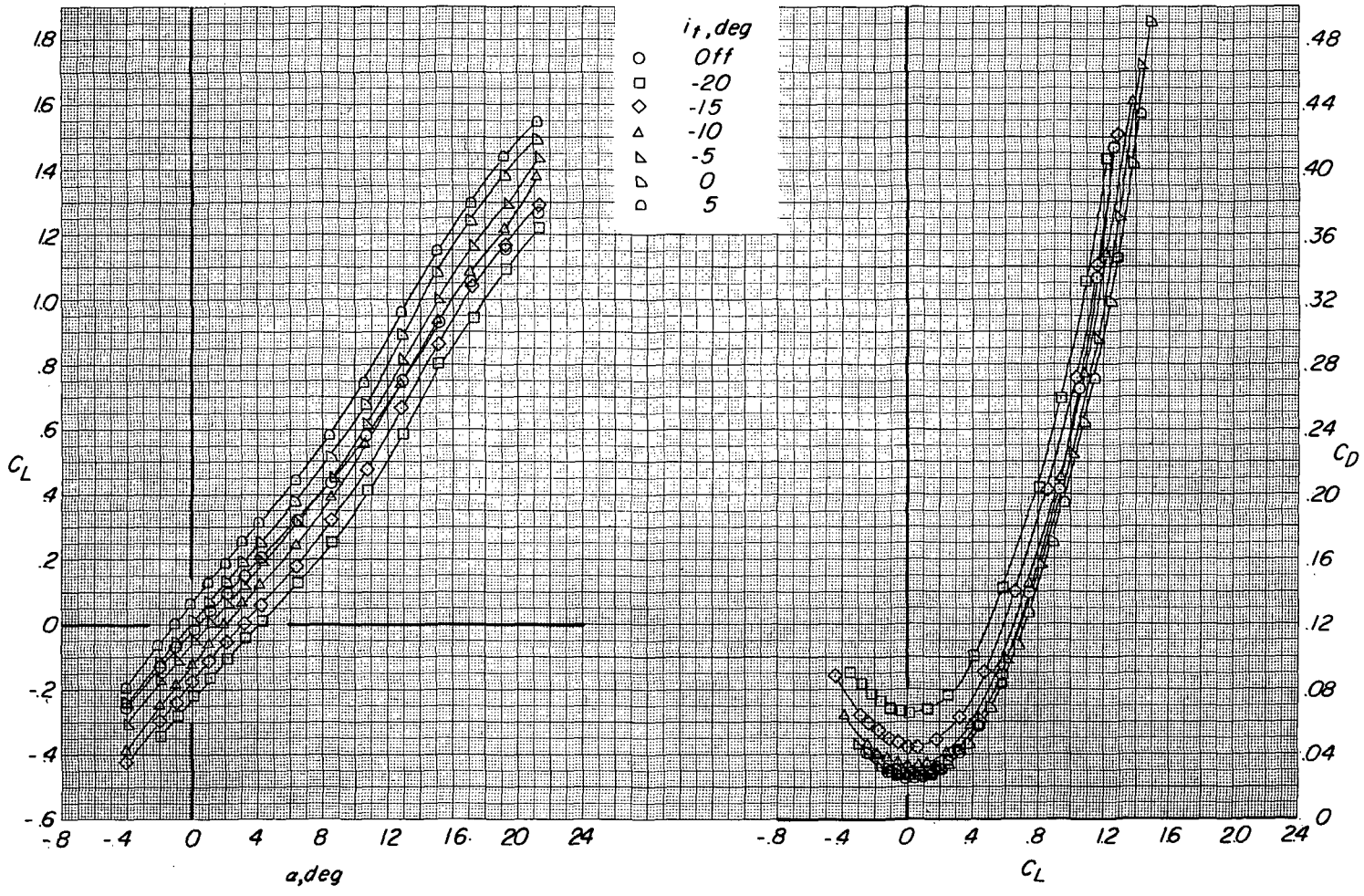

(b) C_L against α and C_D.

Figure 14.- Concluded.

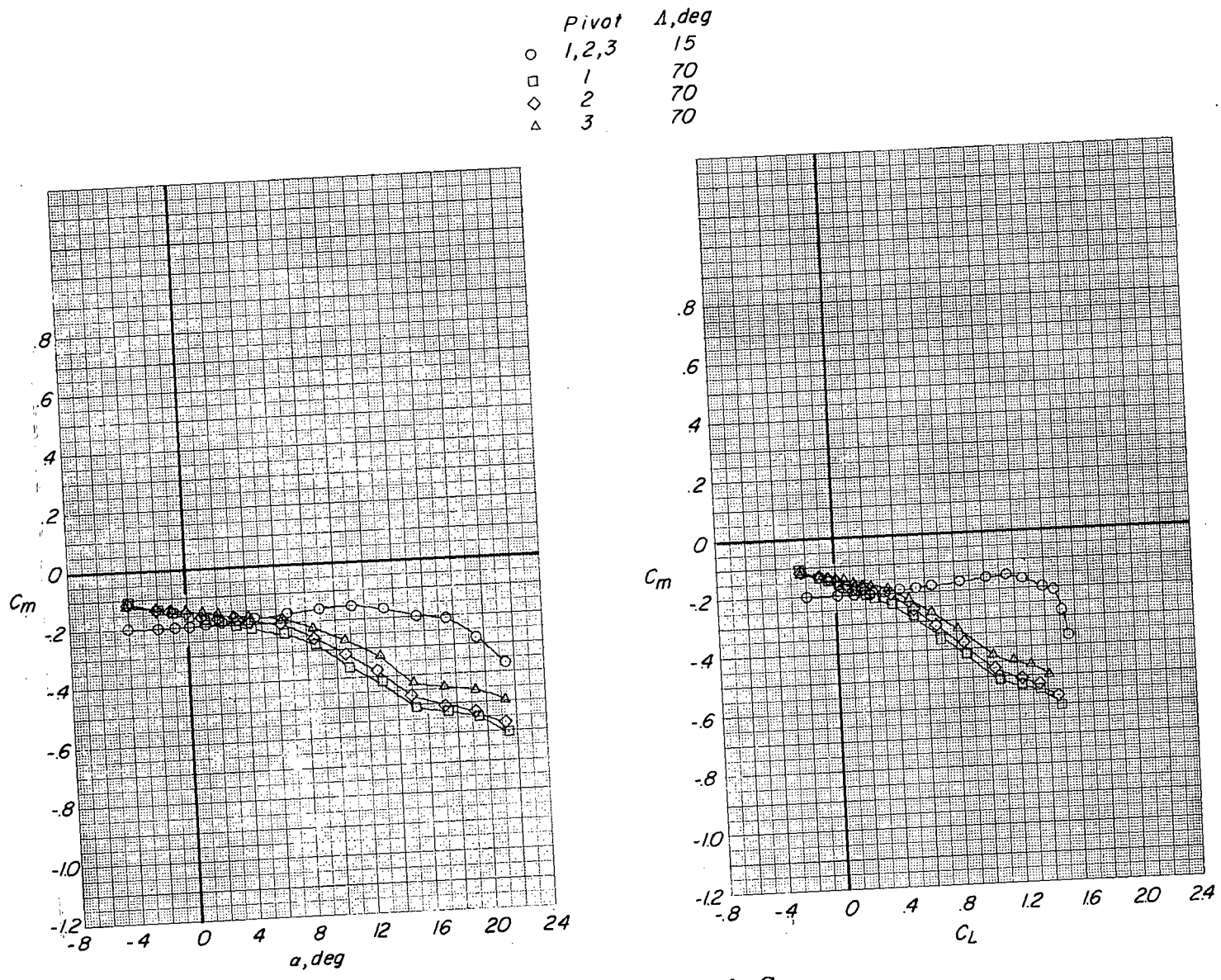

(a) C_m against α and C_L.

Figure 15.- Effect of sweep-angle variation on the aerodynamic characteristics of configurations utilizing pivots 1, 2, and 3. $M = 0.27$; $i_t = 0^o$; forewing configuration B.

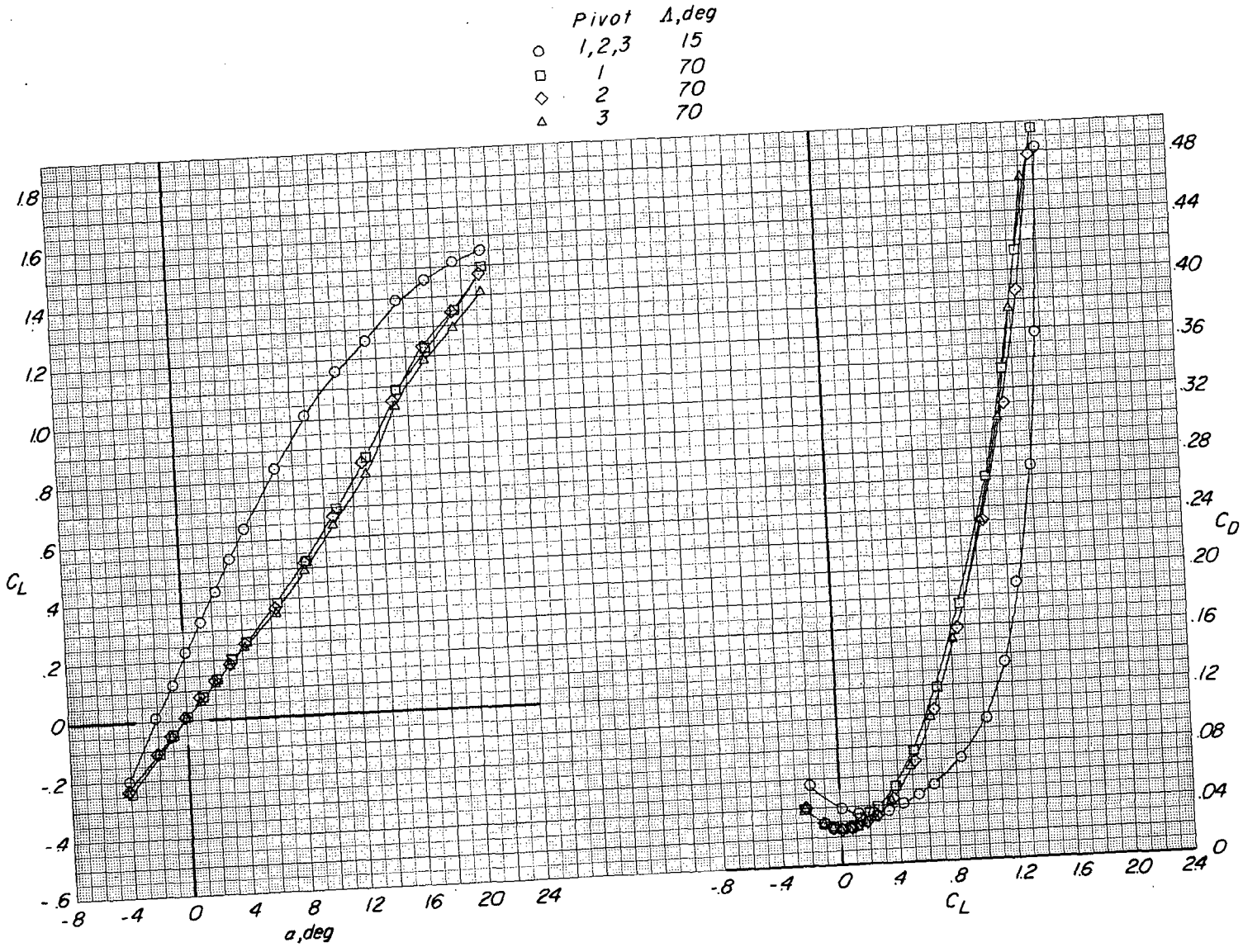

(b) C_L against α and C_D.

Figure 15.- Concluded.

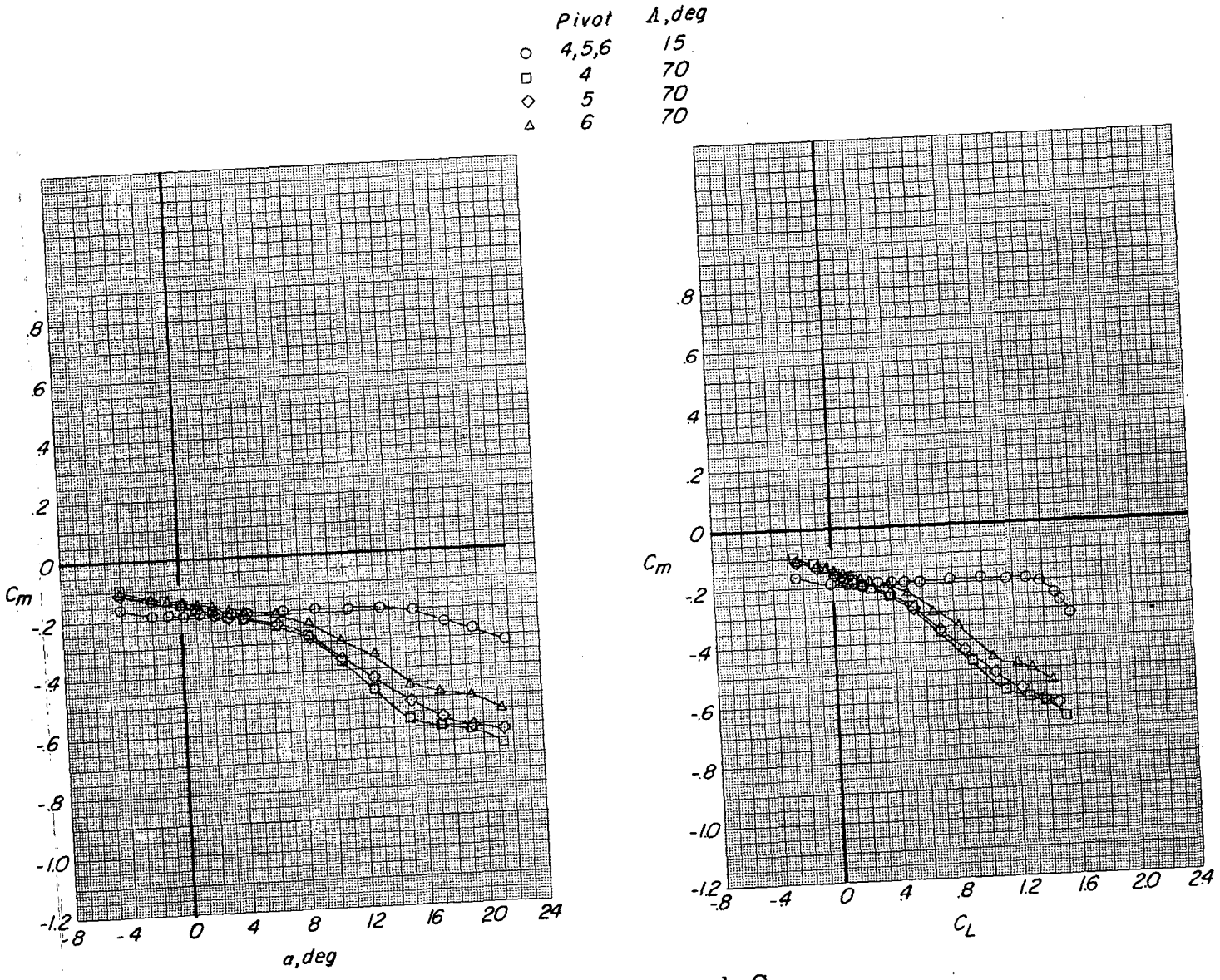

(a) C_m against α and C_L.

Figure 16.- Effect of sweep-angle variation on the aerodynamic characteristics of configurations utilizing pivots 4, 5, and 6. M = 0.27; $i_t = 0^o$; forewing configuration B.

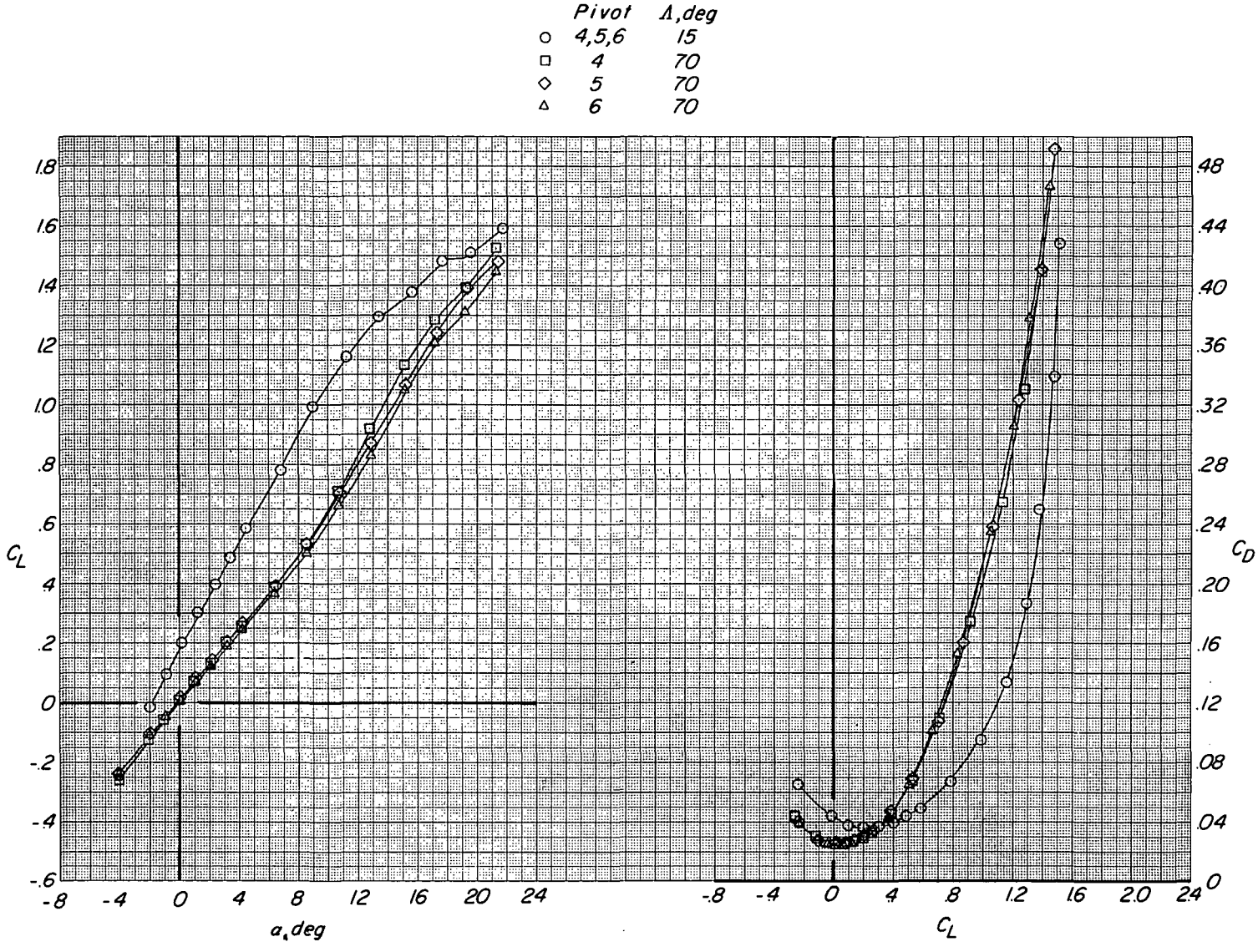

(b) C_L against α and C_D.

Figure 16.- Concluded.

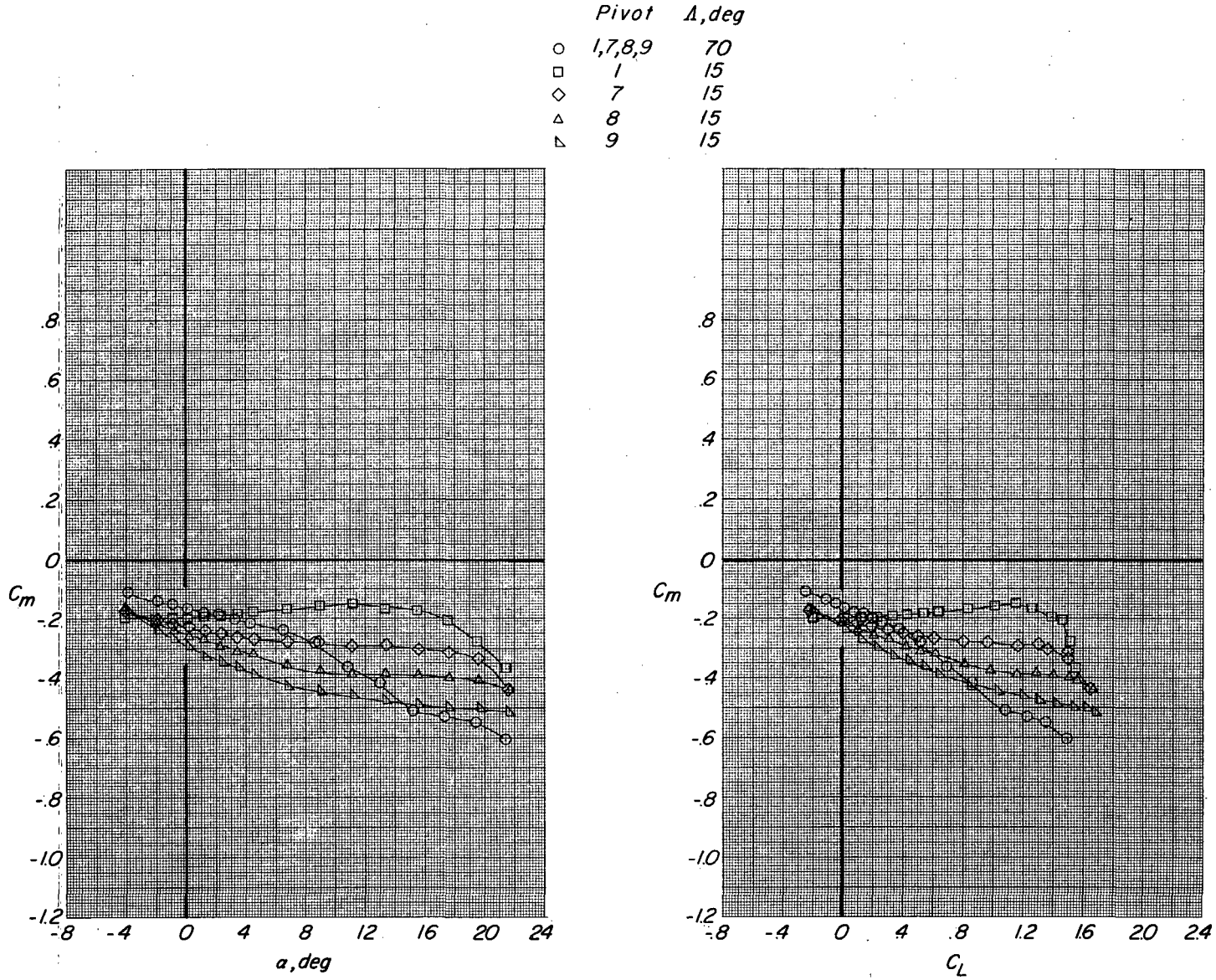

(a) C_m against α and C_L.

Figure 17.- Effect of sweep-angle variation on the aerodynamic characteristics of configurations utilizing pivots 1, 7, 8, and 9. M = 0.27; $i_t = 0^o$; forewing configuration B.

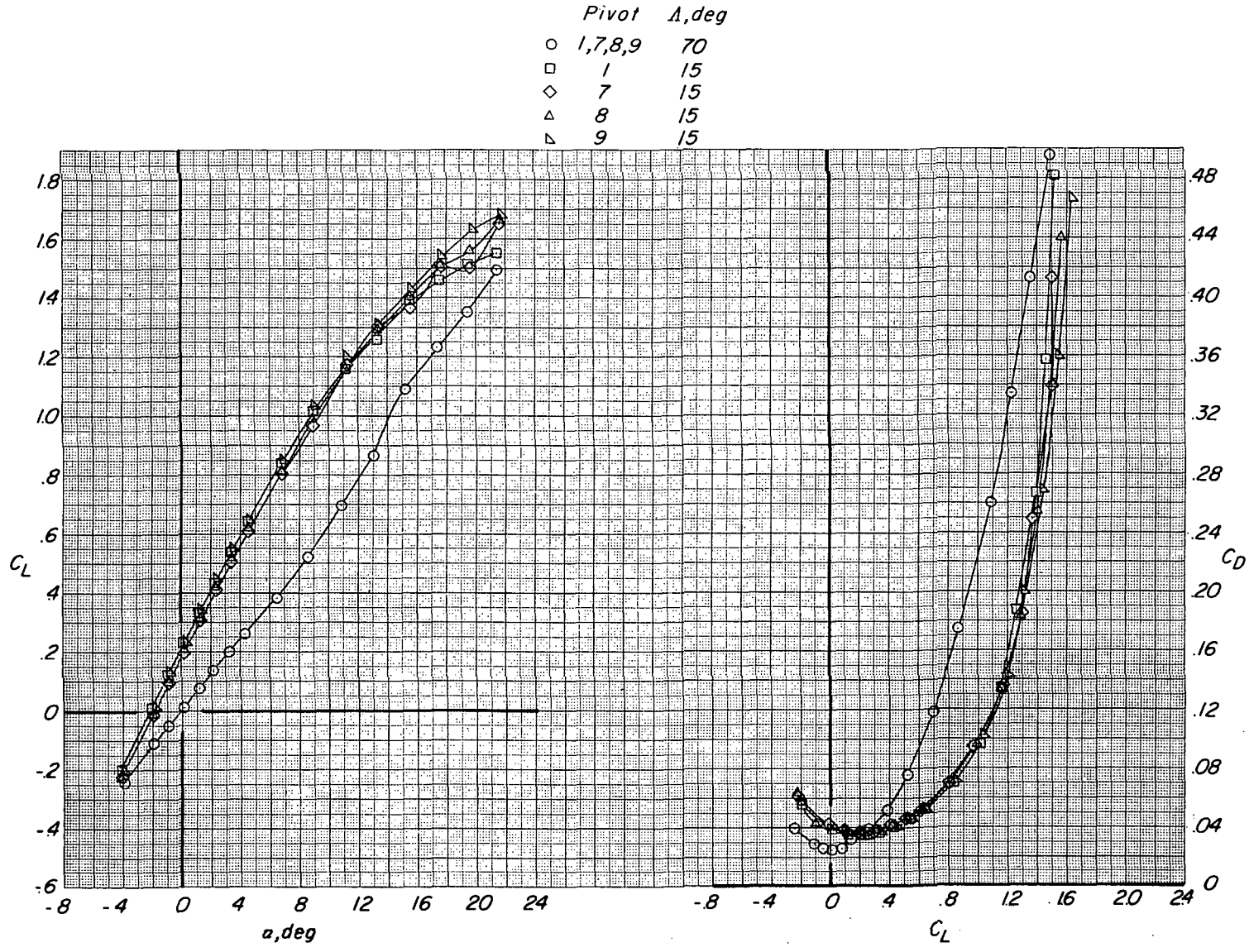

(b) C_L against α and C_D.

Figure 17.- Concluded.

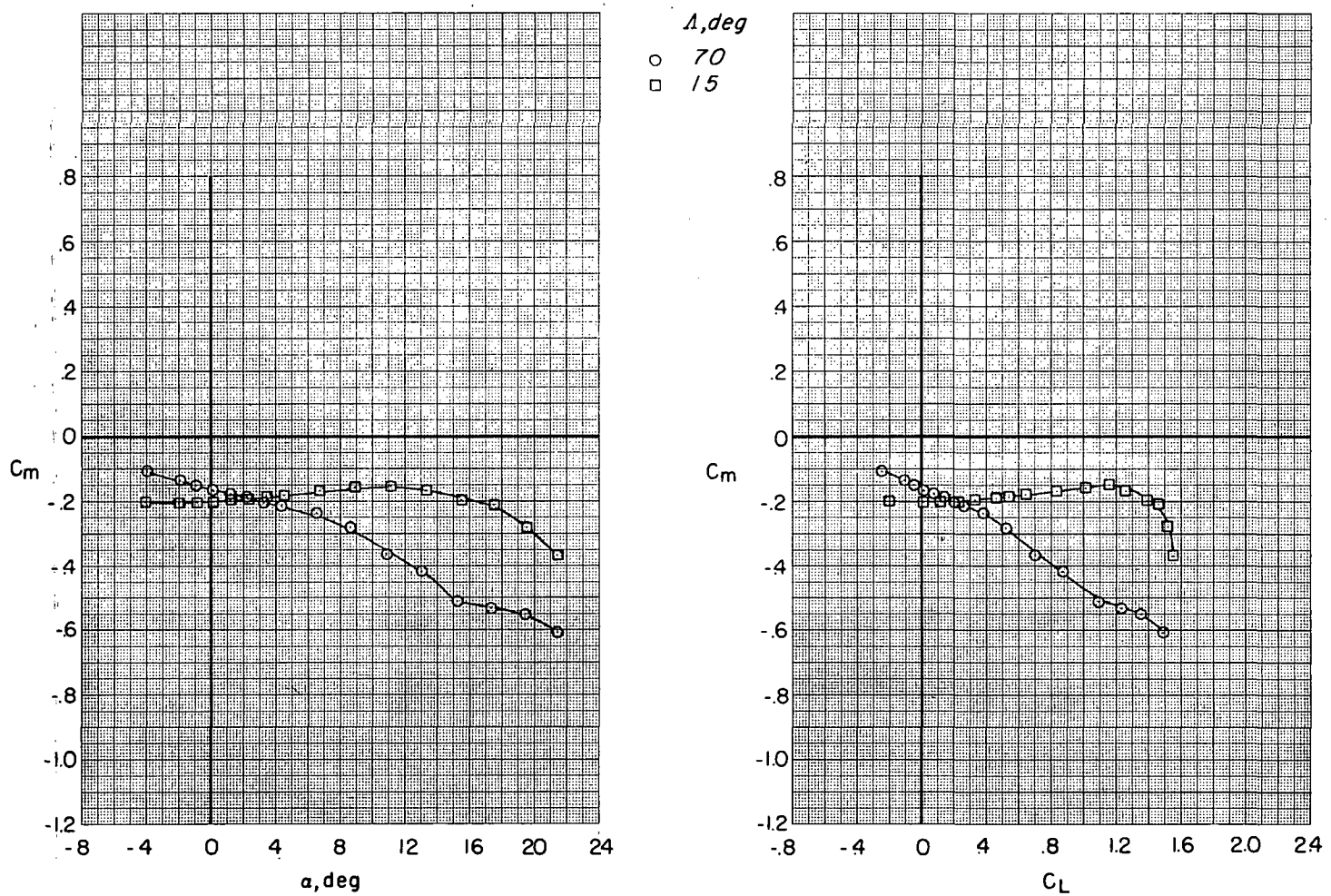

(a) C_m against α and C_L.

Figure 18.- Effect of sweep-angle variation on the aerodynamic characteristics of configuration utilizing pivot 1. M = 0.27; $i_t = 0^o$; forewing configuration B.

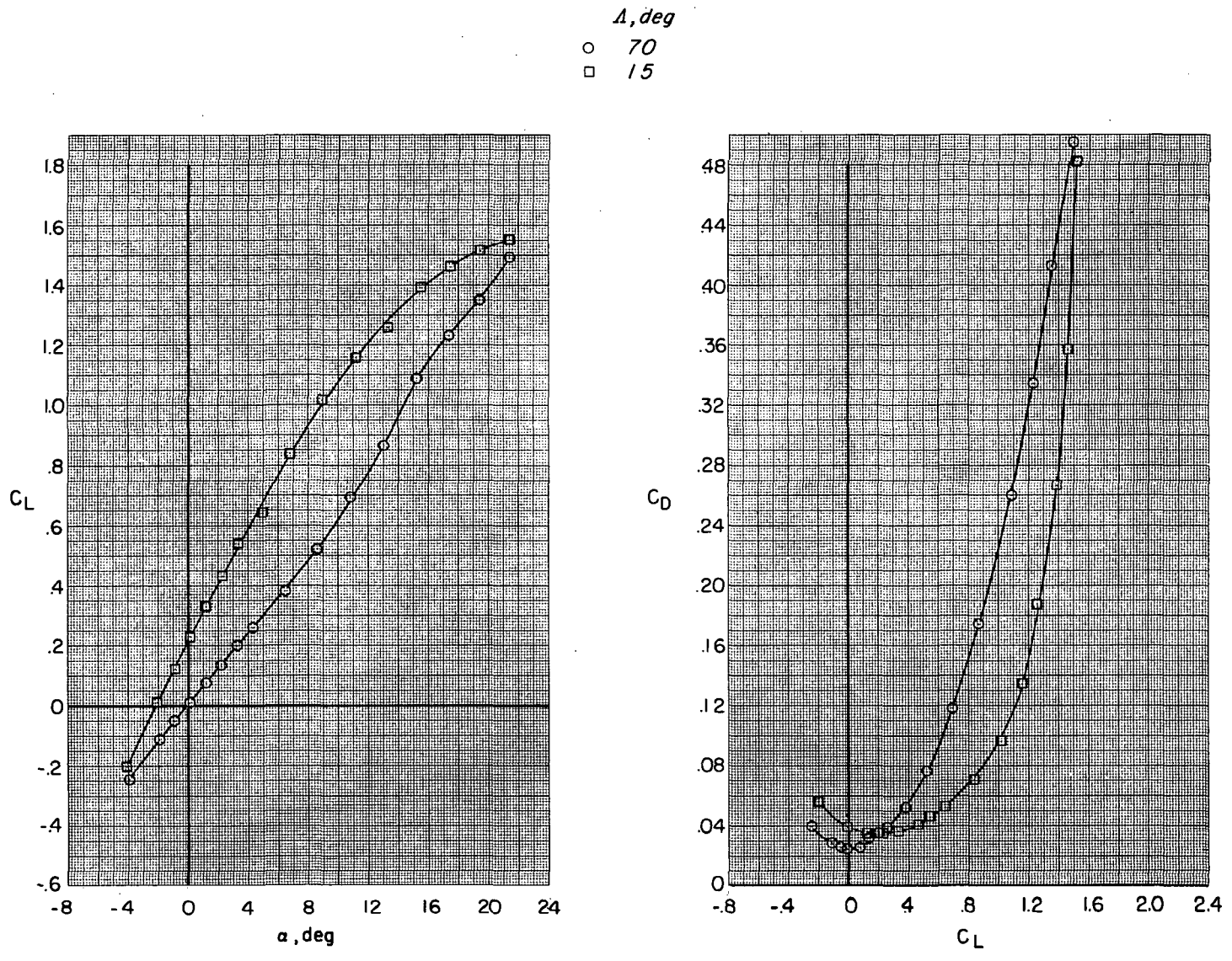

(b) C_L against α and C_D.

Figure 18.- Concluded.

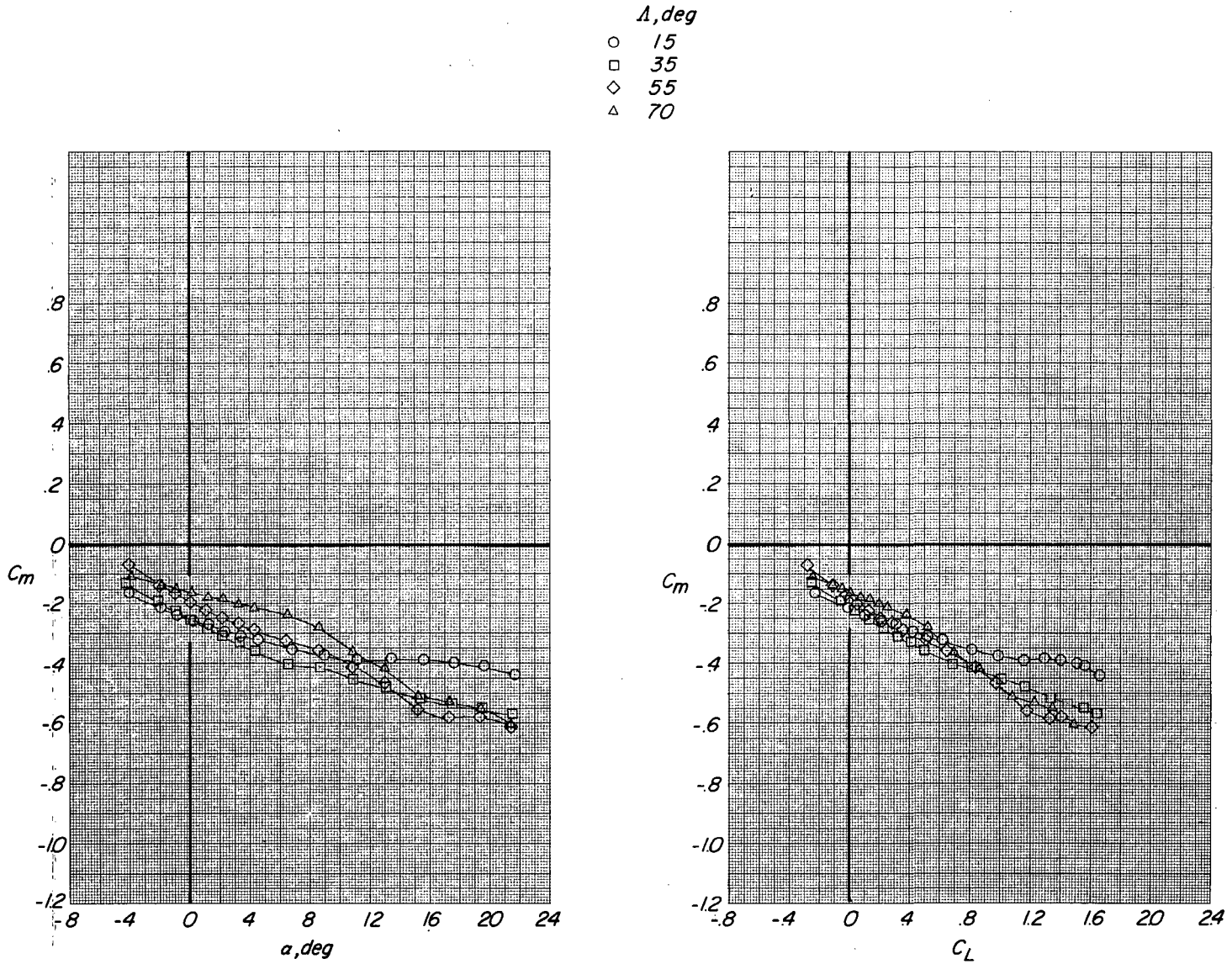

(a) C_m against α and C_L.

Figure 19.- Effect of sweep-angle variation on the aerodynamic characteristics of configuration utilizing pivot 8. M = 0.27; $i_t = 0^o$; forewing configuration B.

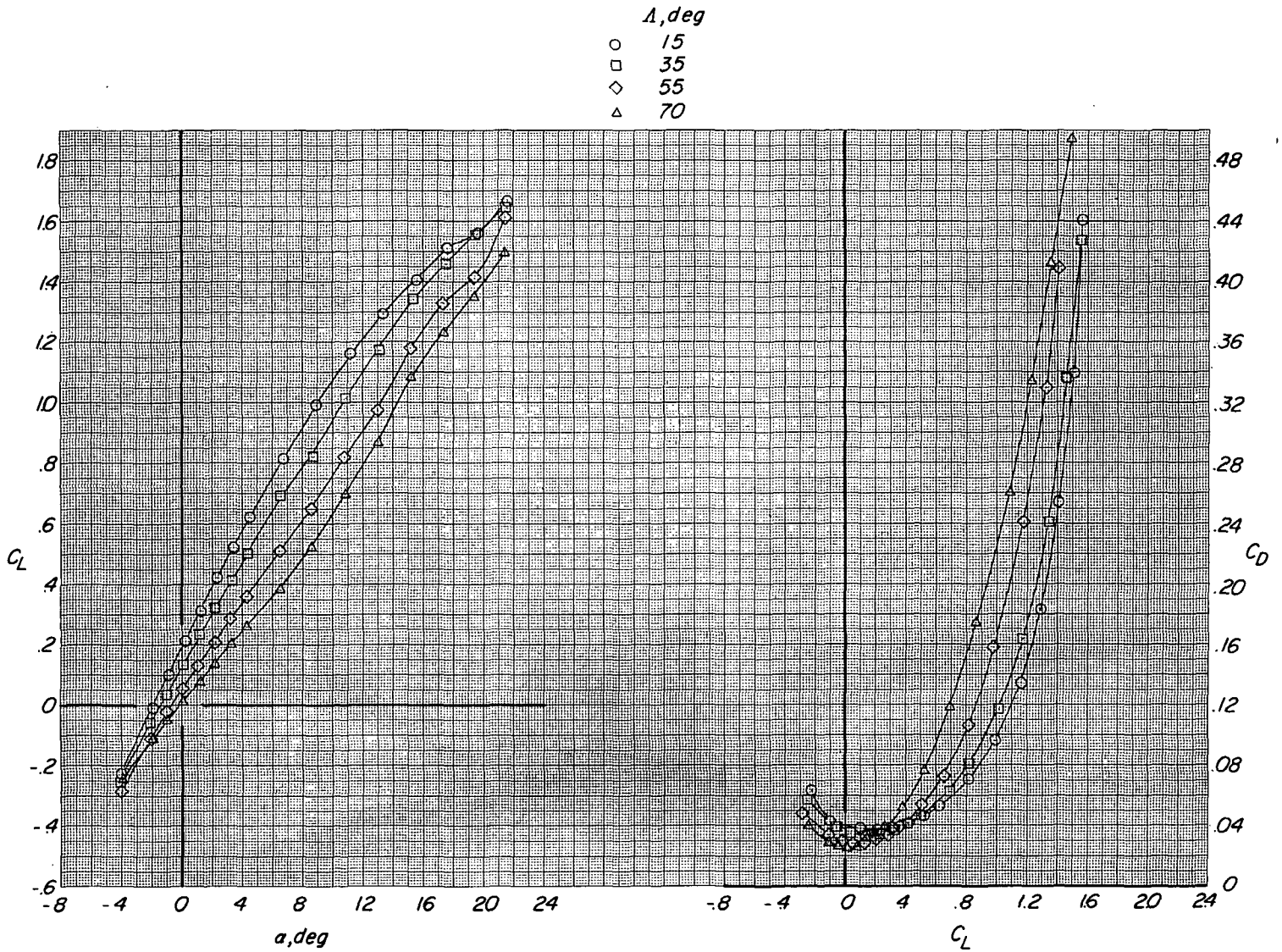

(b) C_L against α and C_D.

Figure 19.- Concluded.

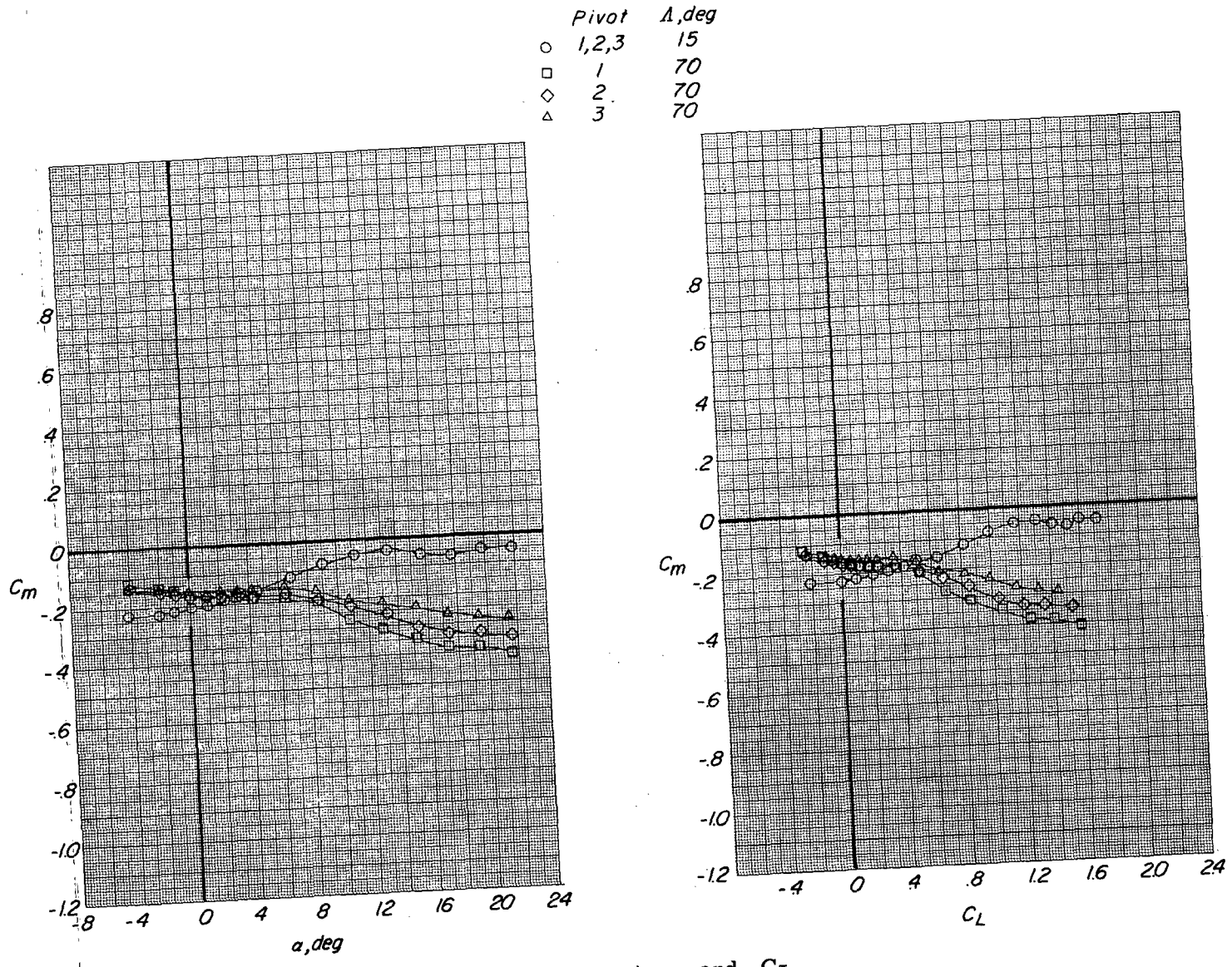

(a) C_m against α and C_L.

Figure 20.- Effect of sweep-angle variation on the aerodynamic characteristics of configurations utilizing pivots 1, 2, and 3. M = 0.27; $i_t = 0^o$; forewing configuration C.

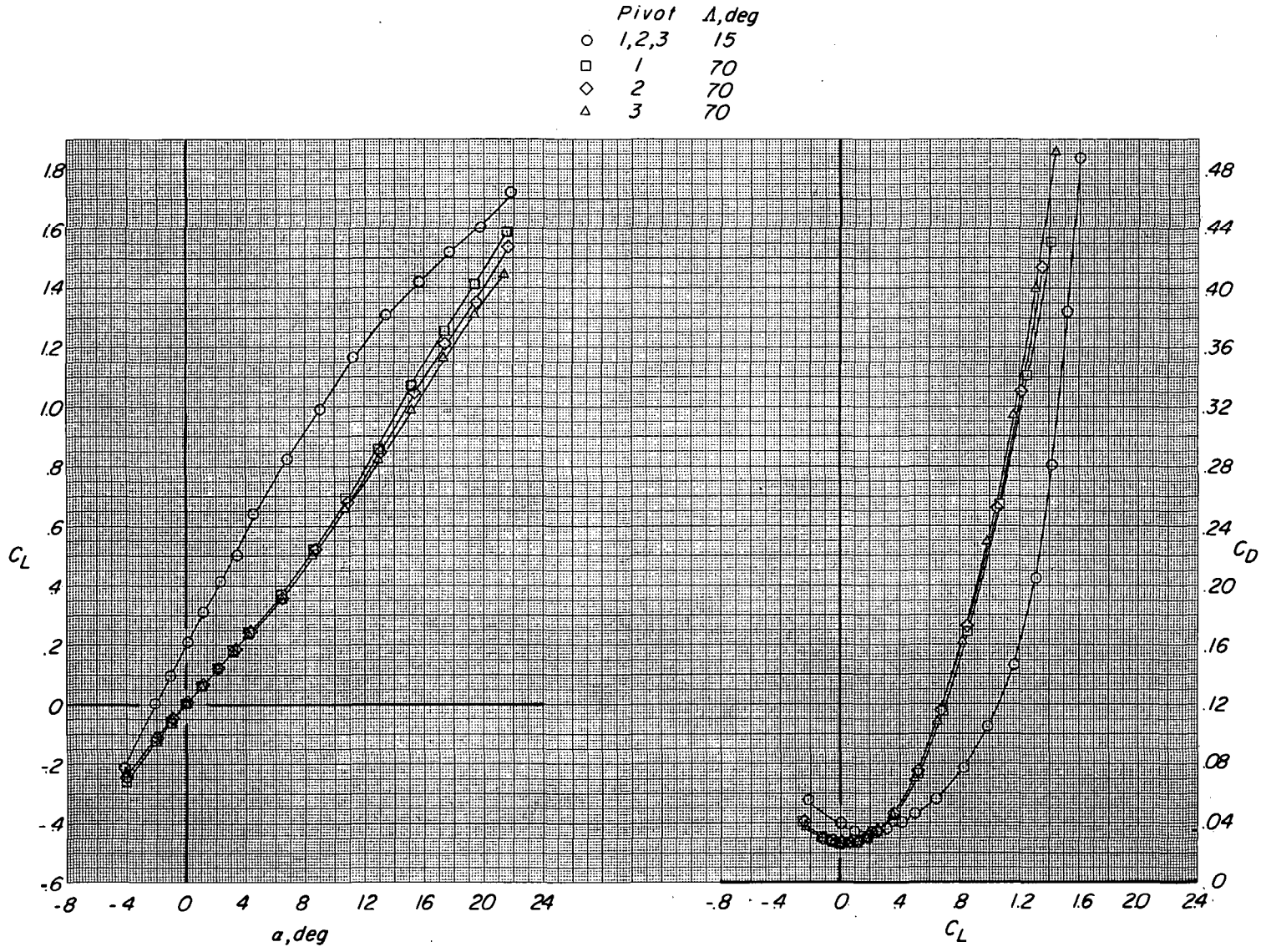

(b) C_L against α and C_D.

Figure 20.- Concluded.

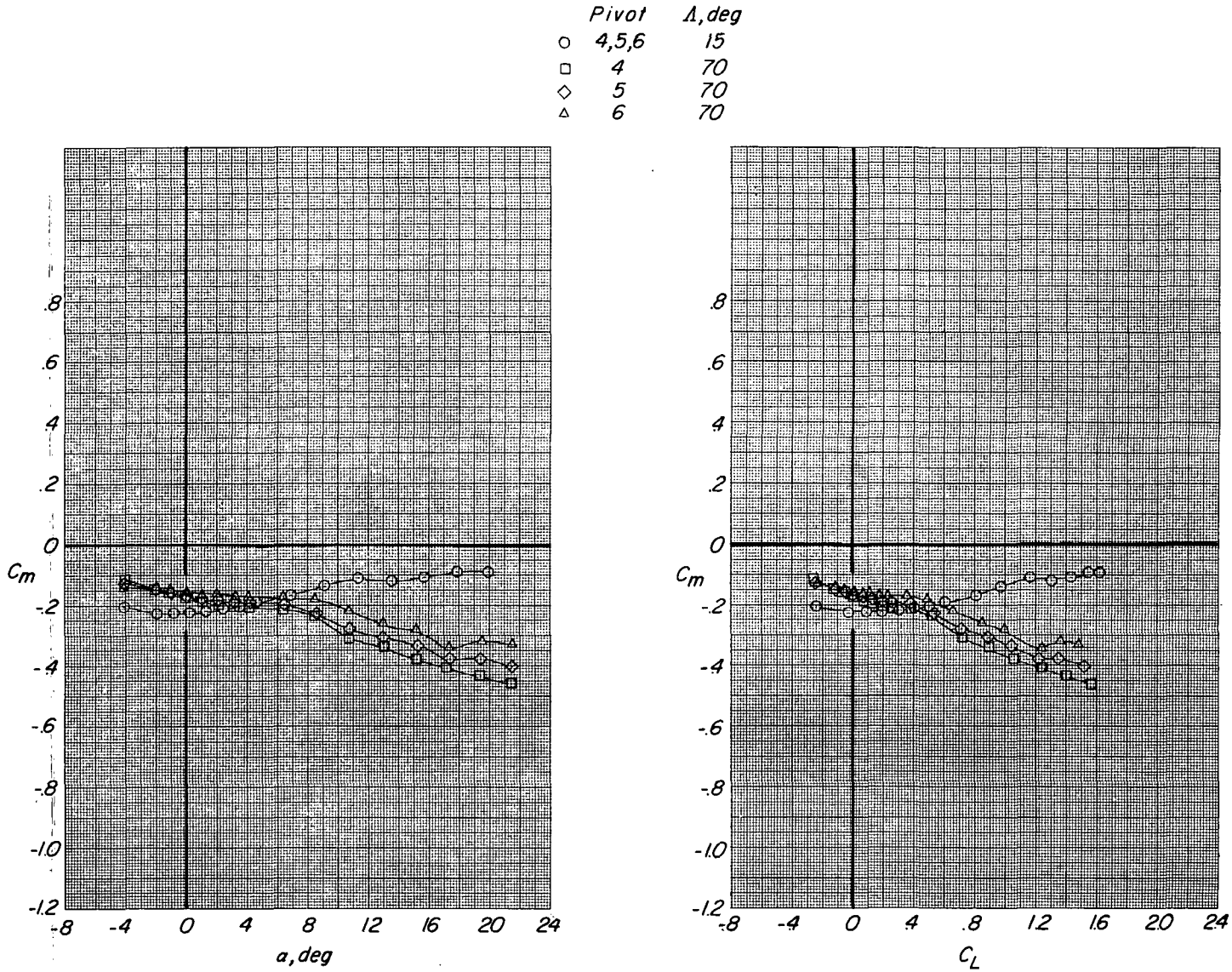

(a) C_m against α and C_L.

Figure 21.- Effect of sweep-angle variation on the aerodynamic characteristics of configurations utilizing pivots 4, 5, and 6. M = 0.27; $i_t = 0^o$; forewing configuration C.

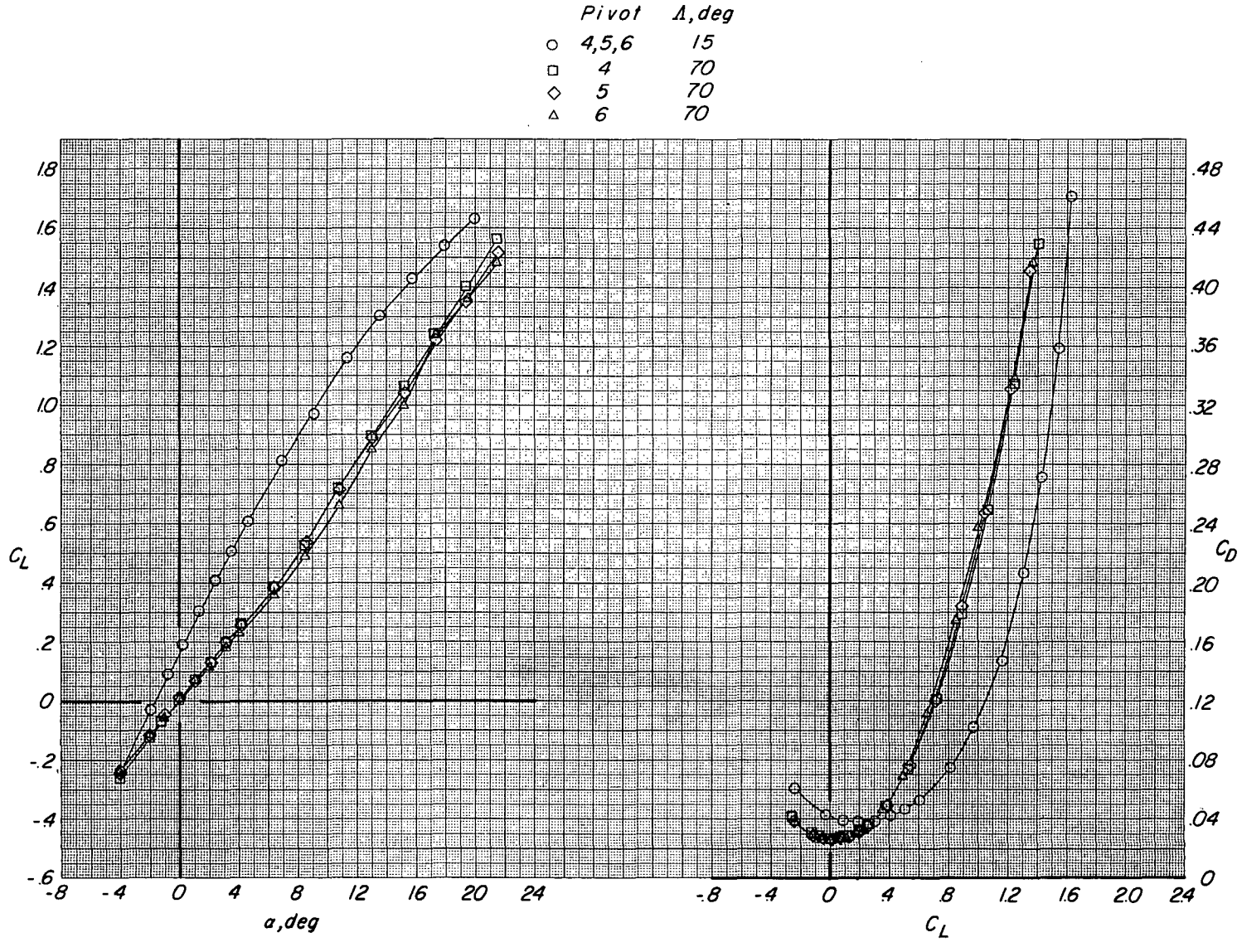

(b) C_L against α and C_D.

Figure 21.- Concluded.

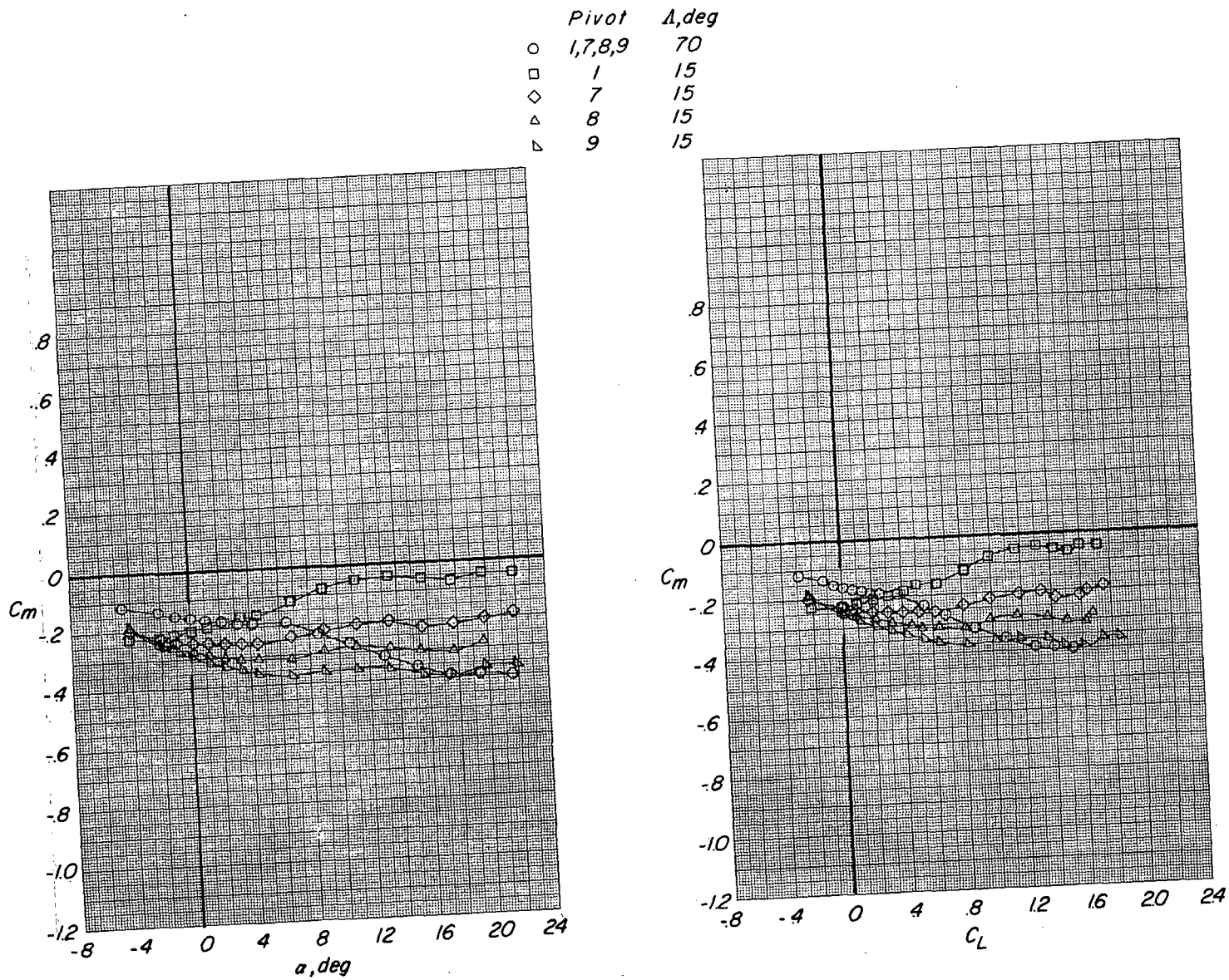

(a) C_m against α and C_L.

Figure 22.- Effect of sweep-angle variation on the aerodynamic characteristics of configurations utilizing pivots 1, 7, 8, and 9. M = 0.27; $i_t = 0^o$; forewing configuration C.

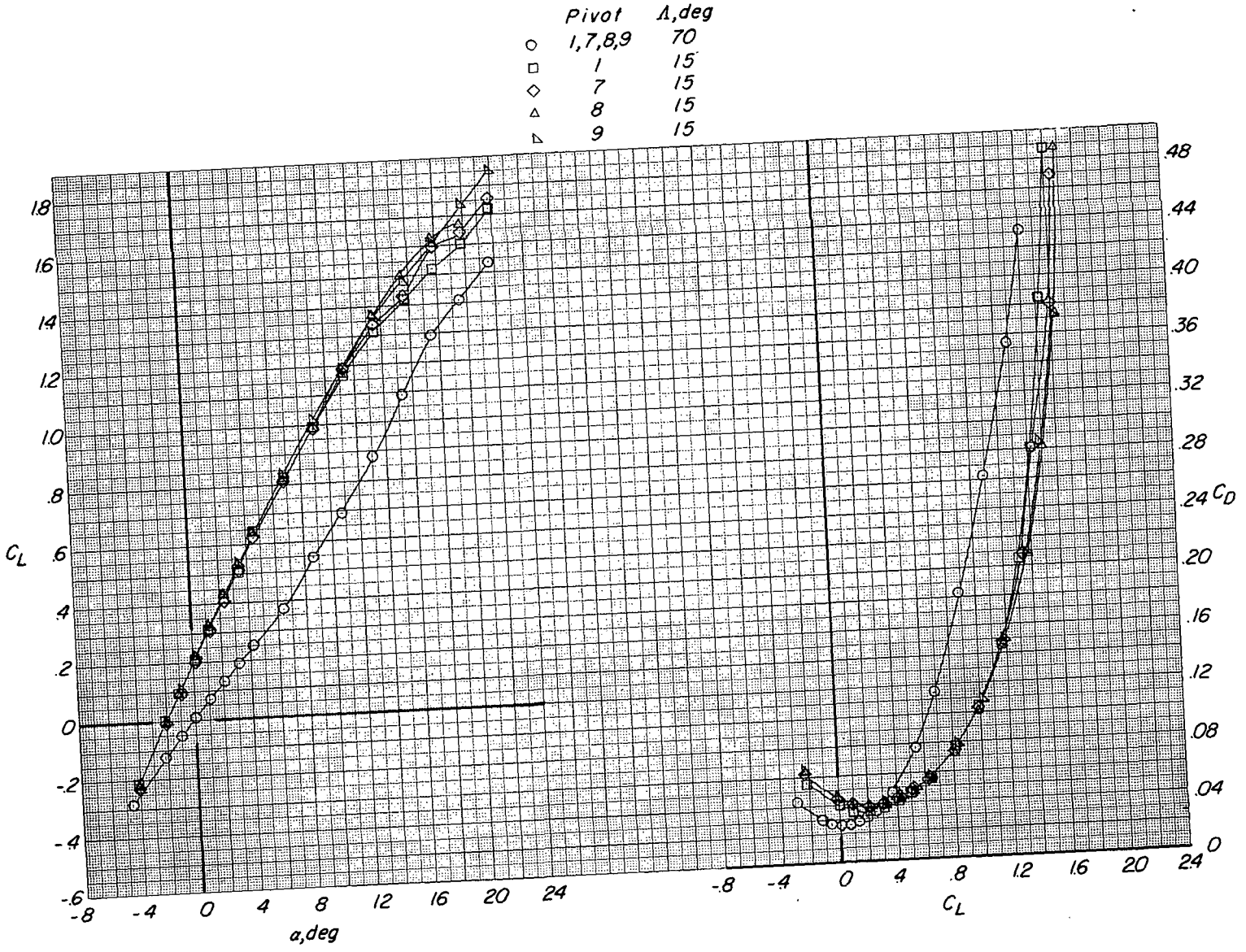

(b) C_L against α and C_D.

Figure 22.- Concluded.

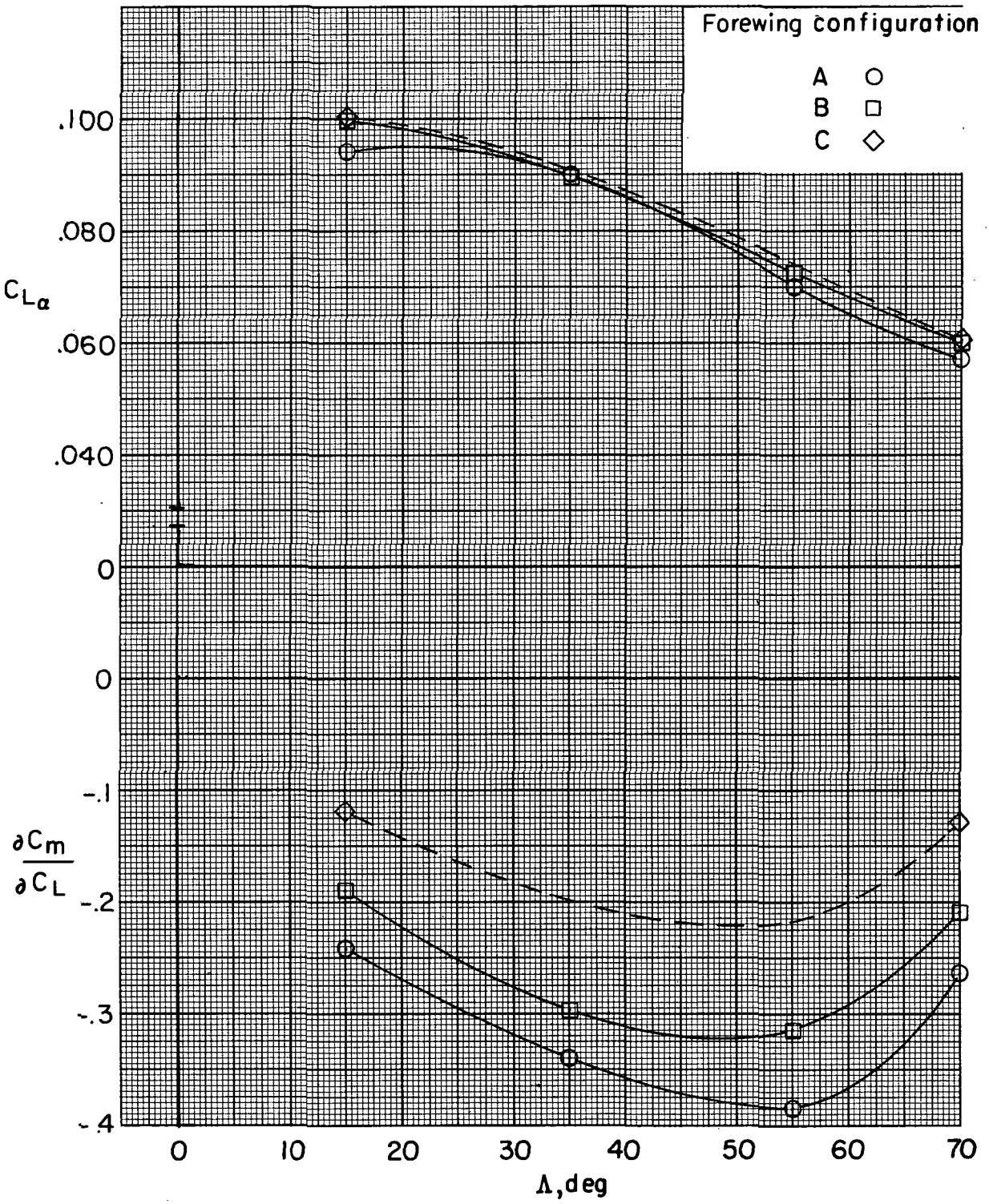

Figure 23.- Lift-curve slope and static margin as a function of wing sweep angle for wing-pivot location 8. Reference forewing area 0.0130 meter (20.1 in.).

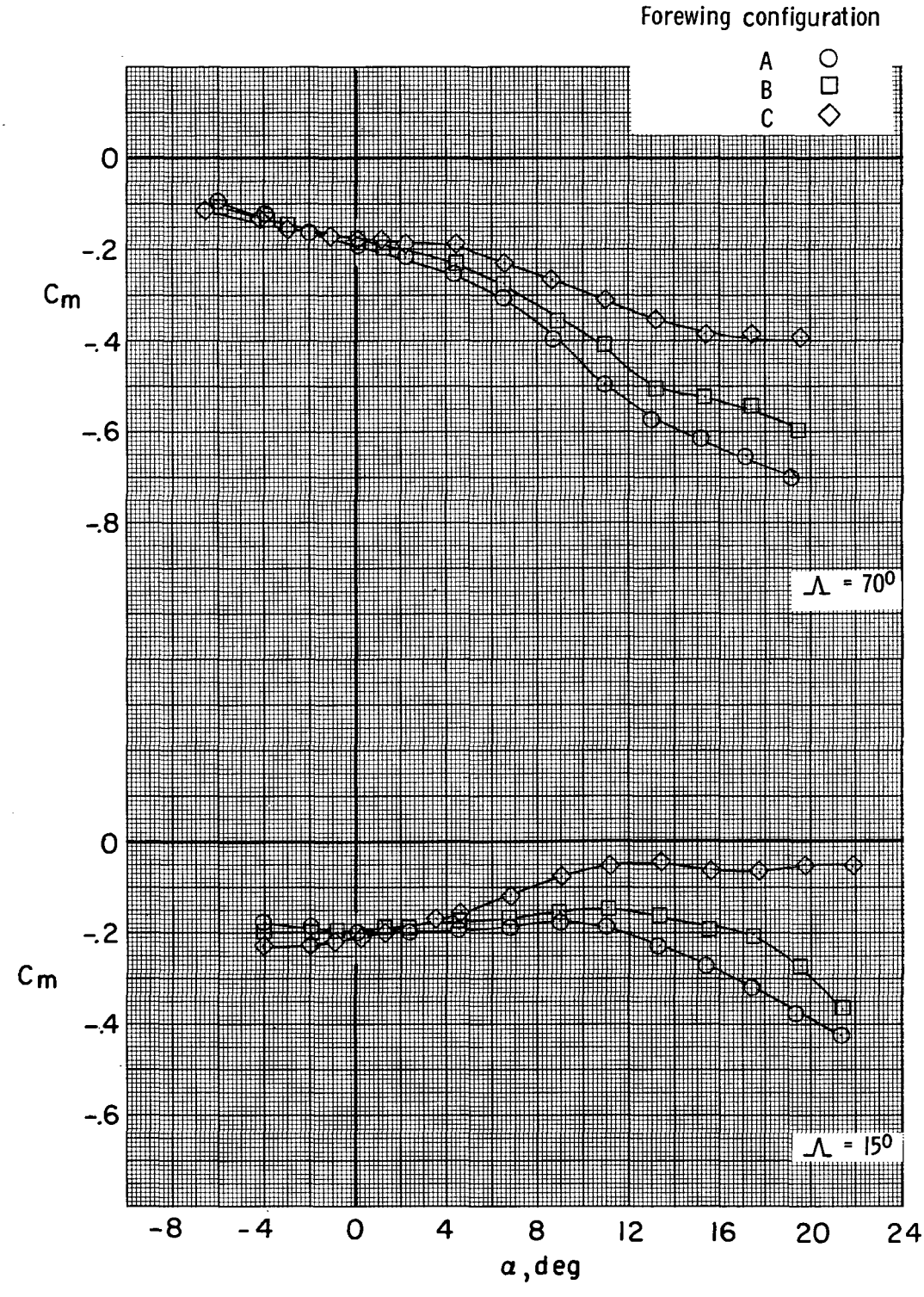

(a) Wing-pivot location 1.

Figure 24.- Variation in pitching-moment coefficient as a function of angle of attack for the three forewing configurations and wing-pivot locations 1 and 8. M = 0.27.

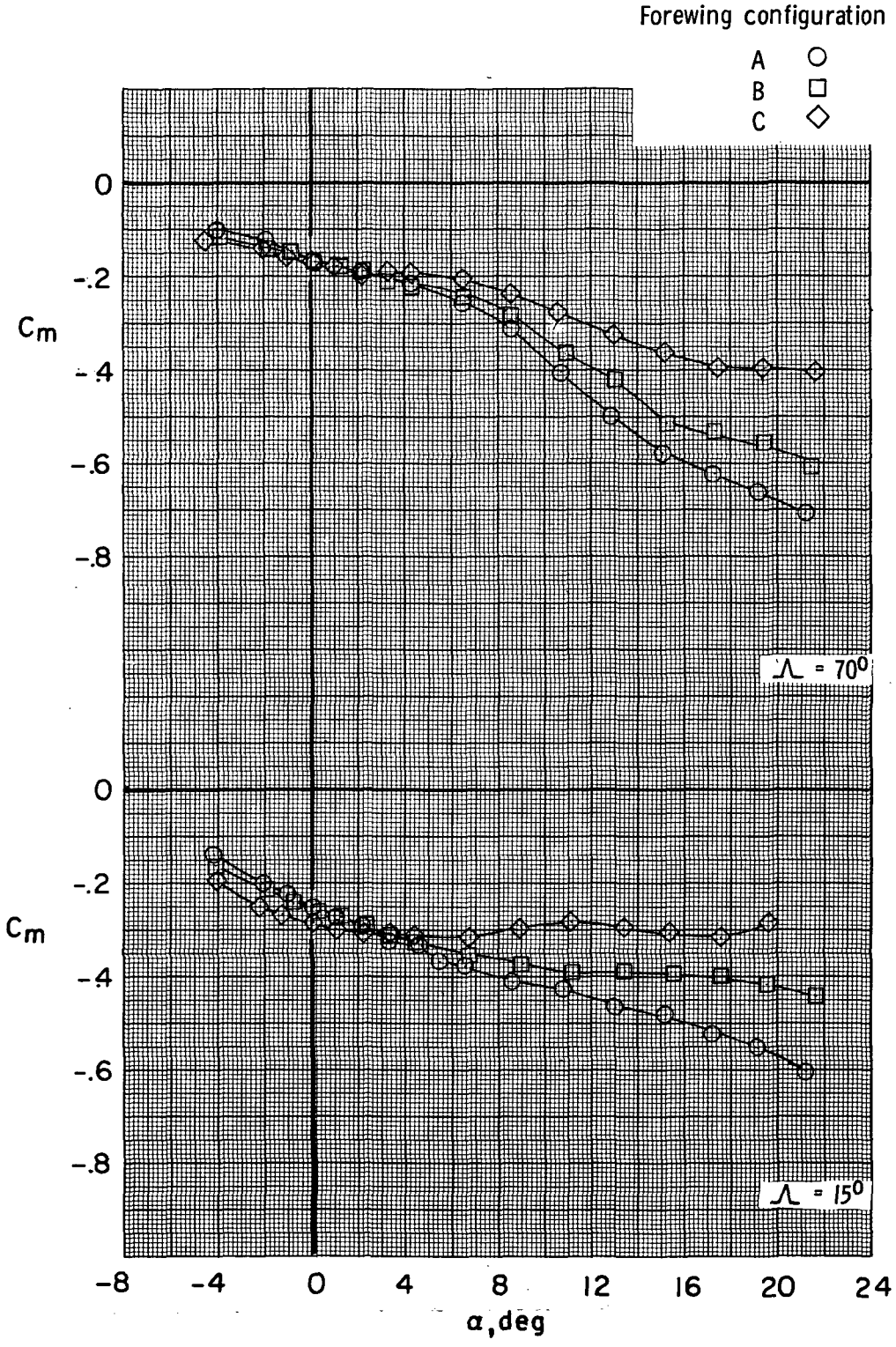

(b) Wing-pivot location 8.

Figure 24.- Concluded.

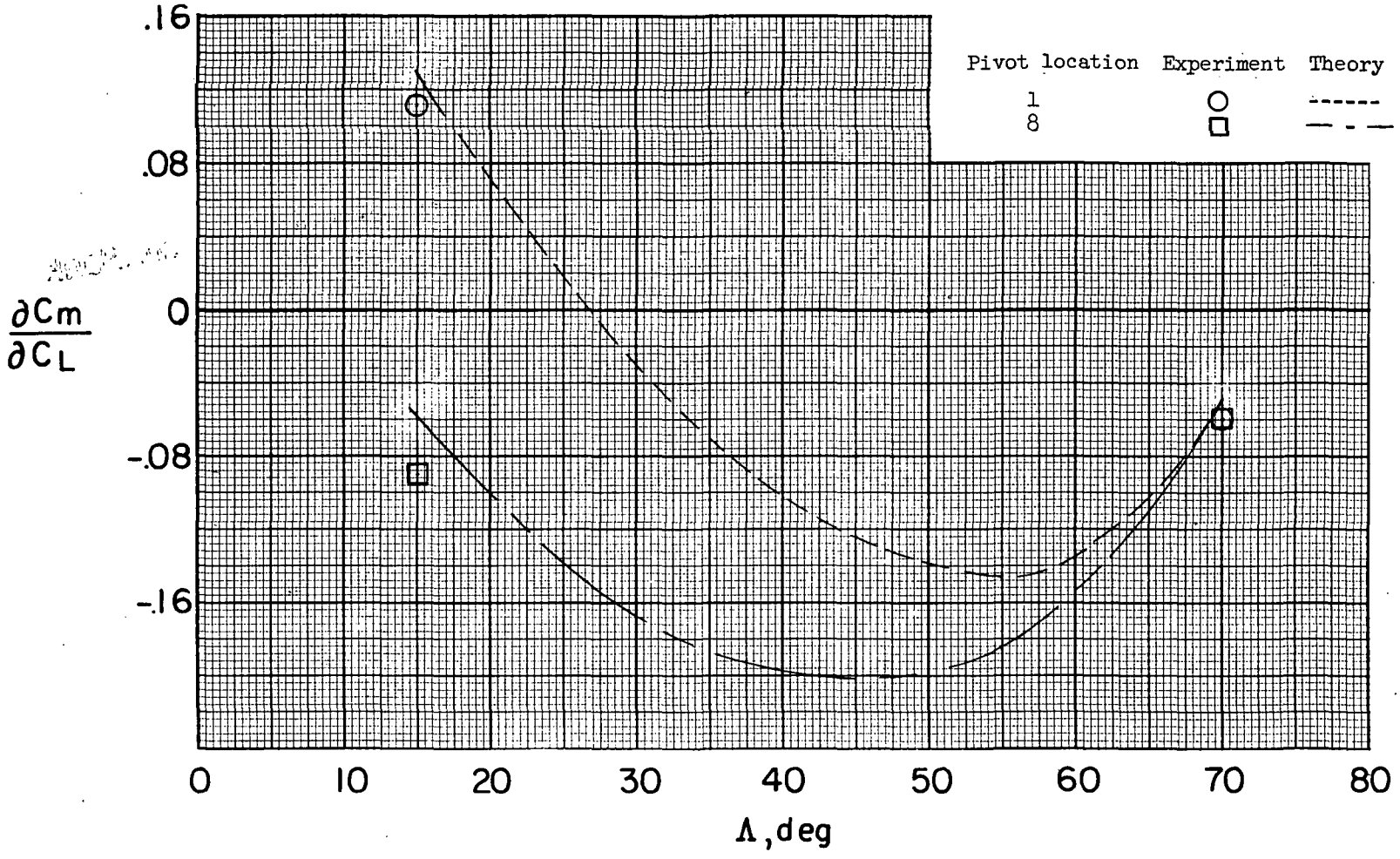

Figure 25.- Variation of static margin with wing sweep angle for wing-pivot locations 1 and 8. M = 0.27; horizontal tail off; configuration C.

NATIONAL AERONAUTICS AND SPACE ADMINISTRATION
WASHINGTON, D.C. 20546

OFFICIAL BUSINESS
PENALTY FOR PRIVATE USE $300

SPECIAL FOURTH-CLASS RATE BOOK

POSTAGE AND FEES PAID
NATIONAL AERONAUTICS AND SPACE ADMINISTRATION
451

U.S.MAIL

POSTMASTER: If Undeliverable (Section 158 Postal Manual) Do Not Return

"The aeronautical and space activities of the United States shall be conducted so as to contribute . . . to the expansion of human knowledge of phenomena in the atmosphere and space. The Administration shall provide for the widest practicable and appropriate dissemination of information concerning its activities and the results thereof."

—NATIONAL AERONAUTICS AND SPACE ACT OF 1958

NASA SCIENTIFIC AND TECHNICAL PUBLICATIONS

TECHNICAL REPORTS: Scientific and technical information considered important, complete, and a lasting contribution to existing knowledge.

TECHNICAL NOTES: Information less broad in scope but nevertheless of importance as a contribution to existing knowledge.

TECHNICAL MEMORANDUMS: Information receiving limited distribution because of preliminary data, security classification, or other reasons. Also includes conference proceedings with either limited or unlimited distribution.

CONTRACTOR REPORTS: Scientific and technical information generated under a NASA contract or grant and considered an important contribution to existing knowledge.

TECHNICAL TRANSLATIONS: Information published in a foreign language considered to merit NASA distribution in English.

SPECIAL PUBLICATIONS: Information derived from or of value to NASA activities. Publications include final reports of major projects, monographs, data compilations, handbooks, sourcebooks, and special bibliographies.

TECHNOLOGY UTILIZATION PUBLICATIONS: Information on technology used by NASA that may be of particular interest in commercial and other non-aerospace applications. Publications include Tech Briefs, Technology Utilization Reports and Technology Surveys.

Details on the availability of these publications may be obtained from:

SCIENTIFIC AND TECHNICAL INFORMATION OFFICE

NATIONAL AERONAUTICS AND SPACE ADMINISTRATION

Washington, D.C. 20546